Developmental Biology 503 (2023) 53–67

Contents lists available at ScienceDirect

Developmental Biology

journal homepage: www.elsevier.com/locate/developmentalbiology

Opposing effects of ecdysone signaling regulate neuroblast proliferation to ensure coordination of brain and organism development

Andreia C. Oliveira, Catarina C.F. Homem *

iNOVA4Health, NOVA Medical School, Faculdade de Ciências Médicas, NMS, FCM, Universidade Nova de Lisboa, Lisboa, Portugal

ARTICLE INFO

Keywords:
Drosophila
Neuroblast
Ecdysone
Brain
Proliferation

ABSTRACT

Growth regulation must be robust to ensure correct final size, but also adaptative to adjust to less favorable environmental conditions. Developmental coordination between whole-organism and the brain is particularly important, as the brain is a critical organ with little adaptability. Brain growth mainly depends on neural stem cell (NSC) proliferation to generate differentiated neural cells, it is however unclear how organism developmental progression is coordinated with NSCs. Here we demonstrate that the steroid hormone ecdysone plays a multi-step, stage specific role in regulating *Drosophila* NSCs, the neuroblasts. We used animals that are unable to synthesize ecdysone, to show that the developmental milestone called "critical weight peak", the peak that informs the body has reached minimum viable weight to survive metamorphosis, acts a checkpoint necessary to set neuroblast cell cycle pace during larval neurogenesis. The peaks of ecdysone that occur post-critical weight are no longer required to maintain neuroblast division rate. We additionally show that in a second stage, at the onset of pupariation, ecdysone is instead required to trigger neuroblast's proliferation exit and consequently the end of neurogenesis. We demonstrate that, without this signal from ecdysone, neuroblasts lose their ability to exit proliferation. Interestingly, although these neuroblasts proliferate for a longer period, the number of differentiated neurons is smaller compared to wild-type brains, suggesting a role for ecdysone in neuron maintenance. Our study provides insights into how neural stem cells coordinate their division rate with the pace of body growth, identifying a novel coordination mechanism between animal development and NSC proliferation.

1. Introduction

To form an organism with the correctly proportionate, stereotypical structures, that are characteristic of each species, animals must tightly regulate body and organ growth during development. However, these growth regulatory processes have to be dynamic enough to allow the animal to adapt to conditions of stress. In fact an animal is capable of slowing down or speeding up development in response to stresses such as nutritional restriction, injury, temperature changes, among others (Colombani et al., 2012; Koyama et al., 2014; Petavy et al., 2001). Delays in development allow for the animal to have enough time to compensate and overcome these stresses and, ideally, successfully reach the adult phase (Boulan et al., 2019; Garelli et al., 2012).

Several genes, signaling pathways and hormones have been implicated in the regulation of organ growth (Nijhout et al., 2014). Organ size can be controlled at the cell autonomous level by adjusting cell growth, cell number/cell division or cell death. An additional layer of regulation occurs at the systemic level, promoted mainly by hormones. This systemic regulation is essential to coordinate the growth between multiple organs, to control developmental progression, durations of growth periods, and to coordinate the growth response to environmental conditions (Droujinine and Perrimon, 2016; Mirth and Shingleton, 2012). How these non-autonomous and autonomous mechanisms interact to coordinate growth in an organ specific manner is however not fully understood.

In *Drosophila melanogaster*, the steroid hormone Ecdysone (ecd) is the central regulator of developmental timing, regulating molting and metamorphosis and therefore growth periods (Quinn et al., 2012). The precursor of ecd is produced in the prothoracic gland (PG) and is modified to its active form, 20-Hydroxyecdysone (20E), in the peripheral tissues (Gilbert, L. I. & Warren, J. T.2005). It is released in pulses throughout development and activates stage-specific gene cascades to drive developmental progression (Thummel, 1996). The PG is part of a larger endocrine structure called Ring Gland which also contains the corpora allata, and the corpora cardiaca (King et al., 1966).

During the third instar larval stage (L3), three small pulses of ecd

* Corresponding author.
E-mail address: catarina.homem@nms.unl.pt (C.C.F. Homem).

https://doi.org/10.1016/j.ydbio.2023.08.001
Received 13 January 2023; Received in revised form 1 August 2023; Accepted 4 August 2023
Available online 6 August 2023

regulate different gene cascades that mark developmental milestones. The first peak marks the reaching of the critical weight (CW) which is the minimal body mass necessary to progress to metamorphosis without a developmental delay, and therefore is sometimes referred as the CW peak. The second larval peak of ecd triggers the expression of glue genes that allow the animal to adhere to vertical surfaces once it forms a pupa, and the third peak marks the start of wandering behaviour, when the animal abandons the food and starts looking for a place to pupariate. In late L3 development a major pulse of ecd, also known as the pupariation peak, initiates puparium formation.

It has been shown that preventing ecd production during L3 stages leads to a developmental arrest preventing the animals from pupariating and going through metamorphosis (Berreur and Porcheron, 1984). Consequently, these larvae continue to grow for as long as three weeks, an age equivalent to a 10-day old adult fly (Oldroyd, 1951). Interestingly, it has been shown that the massive growth of these larvae is not accompanied by a proportional size increase in all organs (Herboso et al., 2015). Epithelial tissues, such as the wing discs, arrest their growth, decreasing their cellular proliferation rates and cell sizes, while the gut continues to increase in size (Herboso et al., 2015). The response to ecd is thus tissue specific. It remains however unclear how overall developmental progression is coordinated at the cellular level, particularly in progenitor cells such as stem cells, which are major drivers of organ formation and growth.

In the brain the coordination of animal development and stem cell proliferation is particularly important as defects in the number of differentiated neurons cannot be easily compensated by, for instance, increases in cell size as happens in epithelial tissues (Neufeld et al., 1998). The *Drosophila* brain is an organ that does not go through metamorphosis and which's growth is dependent on the proliferation of neural stem cells, the neuroblasts (NB) (Bello et al., 2008; Truman and Bate, 1988; White and Kankel, 1978). NBs are generated in the embryo and undergo several waves of proliferation coordinated with the different stages of animal development (Ito and Hotta, 1992). The majority of adult neurons are generated by NBs during larval and early pupal stages and once neurogenesis is complete NBs are decommissioned, a process for which ecd signaling and energy metabolism have been shown to be important (Homem et al., 2014). Blocking ecd signaling in NBs from embryonic stages to pupal stages prevents NB decommissioning, indicating that ecd is necessary for this process. It remains however unclear at which developmental stage this regulation by ecd occurs. The NB decommissioning process is characterized by a metabolic switch from a glycolytic dependent metabolism to rely more on Oxidative phosphorylation (Oxphos). This switch is followed by a progressive reduction in NB size until 24h after puparium formation (APF), when NBs are thought to terminally differentiate (Homem et al., 2014; Maurange et al., 2008). It is, however, not understood how NB proliferative windows and the termination of neurogenesis are so precisely coordinated with overall animal development under normal or stress conditions.

Here we test if and how ecd co-regulates body growth and brain development, specifically by addressing ecd's regulatory role in NBs. Using animals that lack prothoracic glands, we took the approach of removing ecd signaling at key developmental milestones to answer this question.

We have discovered that the CW peak of ecd acts as a checkpoint for NB proliferation by determining the NB cell cycle pace during larval neurogenesis. By ablating the PG at the beginning of the third larval stage (L3), prior to the CW peak, thus preventing ecdysone synthesis thereafter, we observed that NBs proliferate at a slower rate while never ceasing to proliferate.

Interestingly, our findings indicate that it is the ecdysone pupariation peak, occurring during late larval development, that triggers NB size reduction. Normally this reduction leads to the exit from proliferation and the termination of neurogenesis. Our results demonstrate, *in vivo*, that in the absence of ecd, NBs in the central brain have the ability to proliferate indefinitely.

Surprisingly, despite the prolonged proliferation period of NBs, the total number of differentiated cells in the brain is lower compared to wild-type brains. However, we observed no significant increase in apoptosis levels or defects in lineage progression. These results suggest that ecdysone may also play a role in the generation and/or maintenance of neurons, indicating a potential additional function for ecdysone in the neurodevelopmental process.

Overall, our results show that the steroid hormone ecd coordinates brain growth with animal development in a multi-step process and in a stage specific manner, regulating *Drosophila* NB division rate and proliferate periods.

2. Materials and methods

2.1. Fly strains

phmGAL4tubGAL80^{ts} and UAS-Grim were both a gift from C. Mirth lab, Dicer2/hs-hid; AseGAL4 UASCD8GFP/Cyo and UASDicer2/hs-hid; insc-GAL4 UASCD8GFP/CyO were a gift from J. Knoblich (Homem et al., 2014). LexAOP- sti RFP was a gift from C. Mendes. UAS-sti GFP (BDSC_90920), UAS-EcR-DN (dominant negative, BDSC_9452), UAS-EcR RNAi (BDSC_9327) and Dpn LexA (BDSC_52442) were obtained from the *Drosophila* Bloomington Stock Centre.

2.2. Fly rearing and prothoracic gland ablation

Flies were maintained at room temperature and fed on standard fly food medium unless stated otherwise. For ecdysone depletion experiments crosses were placed at 18 °C and larvae reared at this temperature until the 6th day of development, unless stated otherwise. For ablation of the PG, animals were placed at 29 °C until dissection time. All control animals were subjected to the same manipulations and temperature shifts as PG ablated animals. For timed pupal brain dissections, white prepupae were collected and kept at 29 °C until dissection at the stated timepoints.

2.3. L2/L3 collections

On the 6th day of development, all second instar larvae (L2) were collected using a solution of 20% sucrose and placed in a new food plate at 18 °C. Three hours after this collection, all third instar larvae (L3) in those plates were collected to a new plate and placed at 18 °C and, afterwards, moved to 29 °C at the following time points depending on which L3 ecdysone peak was meant to be prevented:

Ablation before the first ecdysone peak - moved to 29 °C immediately after L3 ecdyses;

Ablation before the second ecdysone peak - moved to 29 °C 24h after L3 ecdyses (equivalent to 12h AL3e if animals were reared at 25 °C);

Ablation before the ecdysone pupariation peak – moved to 29 °C 64h after L3 ecdyses (equivalent to 32h AL3e if animals were reared at 25 °C);

Ablation after ecdysone pupariation peak – moved to 29 °C at 0h after puparium formation.

2.4. Immunohistochemistry

Staged animals were dissected in PBS. After dissection, brains were fixed in 4% paraformaldehyde (PFA) in PBS (100–200 μL) for 30 min at room temperature. After this, brains were washed three times with PBS-0.1% Triton X-100 (PBT) at room temperature and blocked for 20 min to 1 h with PBS, 0.1% Triton X-100, 1% normal goat serum (NGS) (blocking solution) at room temperature. The brains were incubated in a total volume of 50 μL of primary antibody, which was diluted in blocking solution, and kept at 4 °C overnight. On the following day, the brains were washed quickly three times using the blocking solution, and

then incubated at room temperature for 20 min to 1 h in blocking solution. Subsequently, the brains were incubated with a secondary antibody, which was diluted in the blocking solution, at room temperature for 2 h while being protected from light. Afterwards, the samples were washed three times with PBT at room temperature, followed by a 10–20 min wash with PBS. The brains were mounted on microscope slides using aquapolymount (Polysciences, Inc).

2.5. NB dissociation and primary cell cultures

Cell dissociation and primary cells culture was done as previously described by (Homem et al., 2013). After L3 staging, 0hL3 larvae were collected and washed once in phosphate-buffered saline (PBS), dissected in supplemented Schneider's medium (10% fetal bovine serum, L-Glutamine 20 mM, L-Glutathione 5 μg/ml, Insulin 20 μg/ml, Schneider's medium (GIBCO)) with or without 20-Hydroxyecdysone (20HE, 5 μg/ml, Sigma Aldrich). For cell dissociation, dissected brains were incubated in Schneider's medium (with or without 20HE) with 1 mg/ml collagenase I and 1 mg/ml of papain (Sigma Aldrich) for 1 h at 25 °C. Brains were washed three times in Schneider's medium with or without 20HE. Brains were manually disrupted with a siliconized pipette tip (VWR) in 50 μl supplemented Schneider's medium with or without 20HE. The dissociated brains were plated in 0.01% poly-L-lysin-hydrobromide coated 4 chamber glass bottom cell culture dishes (Greiner Bio-One) and allowed to settle for 1 h at RT, protected from light. Before imaging, 1 mL of primary cell-culture Schneider's medium with or without 20HE was added to each chamber and imaging was performed immediately.

2.6. EdU incorporation assay

EdU incorporation was performed using the Click-iT EdU Alexa Fluor 647 Imaging Kit (Invitrogen C10340). Staged animals were dissected in Schneider media (SM) (Gibco, 11720-067). After dissection brains were incubated in 100 μM EdU + SM solution for 20min. EdU-labelled brains were fixed in 4% paraformaldehyde (PFA) in PBS (100–200 μL) for 30 min, followed by the immunohistochemistry protocol as described above. For EdU detection, brains were incubated with Click-iT reaction cocktail (Click-iT reaction buffer + CuSO4+Alexa Fluor 647– azide + Reaction buffer additive, prepared in accordance with manufacturer's instructions) for 30 min followed by 3 washes with PBT and a 10 min wash with PBS, all at room temperature. Brains were mounted in aquapolymount (Polysciences, Inc) on microscope slides.

2.7. Antibodies

The following antibodies were used: Rabbit anti-Miranda (1:1000), Guinea pig anti-Miranda (1:200, a gift from J. Knoblich), Rabbit and Mouse anti-PH3 (1:1000, Millipore), Rat anti-Elav (1:100, deposited in DSHB by Rubin, G.M. (DSHB Hybridoma Product Rat-Elav-7E8A10 anti-Elav)), Mouse anti-Repo (1:100 deposited in DSHB by Goodman, C. (DSHB Hybridoma Product 8D12 anti-Repo)) Rabbit anti Dcp-1 (1:100, cell signalling). The following Conjugated secondary antibodies were used: goat anti-rabbit and anti-mouse Alexa fluor 405, goat anti-rabbit, anti-rat, and anti-guinea pig Alexa fluor 568, goat anti-mouse, anti-rabbit and anti-rat Alexa fluor 488 e goat anti-rabbit Alexa fluor 647 (1:1000, Molecular Probes).

2.8. Image acquisition and analysis

Immunofluorescent Z-stack images of brain lobes in posterior and anterior sides were acquired using confocal microscopes LSM710 and LSM880 (Carl Zeiss Microscopy GmbH). Images were processed using the image analysis software FIJI, and Imaris (Bitplane). A minimum number of 5 brain lobes were quantified, unless stated otherwise.

For the quantification of Dcp-1 staining in the entire PG, the maximum intensity value was obtained in FIJI by delimiting the area of the PG using the "free hand" tool and measuring the maximum intensity value within that area. To obtain background signal, a region without Dcp-1 signal was located in the brain and maximum intensity value from that area was subtracted to the one obtained in the PG.

The quantifications of PG cell number and Dcp-1 positive cells were done manually using FIJI. A cell was considered positive for Dcp-1 when its maximum intensity was at least 10 times the mean value of maximum intensity of control PGs.

The measurements of NB diameter and the quantifications of NB number and PH3+ cells per lobe were done manually using the analysis software FIJI. Quantifications of neuron and glial cell number were done using Imaris software "spots" feature (Bitplane). Unpaired T test, or one-way ANOVA were performed to determine statistical significance. Graph production and statistical analysis were achieved using the software GraphPad Prism (Graphpad Software, La Jolla, CA).

Live imaging of cultured cells was performed using an Axio Observer. Z1/7 spinning-disc confocal system (Carl Zeiss Microscopy GmbH). Multiple positions were acquired simultaneously, at each position Z-stacks with 40 μm at 4.4 μm intervals were captured every 6 min. Cell cycle times were determined as the time between two subsequent nuclear envelope breakdowns.

2.9. RNA extraction and qPCR

mRNA from staged animals, 4h after temperature shift, was isolated using TRIzol™ LS Reagent (Invitrogen™) according to the manufacturer's instructions, adjusted for a small amount of RNA. Afterwards, RNA was treated with TURBO DNA-free™ Kit (Invitrogen™) and cDNA was synthesized using the RevertAid First Strand cDNA Synthesis Kit (Thermo Scientific™).

The following primers were used for amplification (as described in Homem et al., 2014):

Act5C—fw: GATAATGATGATGGTGTG CAGG; rv: AGTGGTGGAAG TTTGGAGTG
Eig71Eb—fw: GTCGGCGAACACAAAGAAAT; rv: CGCAGGACAACG TGTTACAT
Eig71Ef—fw: CAGATACATCTGGAAGAATCAGAC; rv:GTTTCCTCT TGTGAGCACTG

qPCRs were performed using GoTaq qPCR Master mix (Promega) on a QuantStudio™ 5 Real-Time PCR System (Applied Biosystems™). The expression of all genes was normalized to Act5C and relative mRNA levels were calculated against control (PhmGAL4TubGAL80ts x UAS-sti GFP) using the $2^{(-\Delta\Delta Ct)}$ method (Livak and Schmittgen, 2001). All experiments were done with technical triplicates.

3. Results

3.1. Ablation of ecdysone production at early L3 stage leads to NBs that do not cease to proliferate

To address if ecd co-regulates the growth of the animal and NB proliferation, we conducted an analysis focused on central brain NBs when ecd signaling was disrupted before the CW peak. To systemically block ecd signaling we induced apoptosis of the PG at the start of L3 development stage (0 h after L3 ecdysis, 0 h AL3e). To eliminate the PG we used a genetic combination to induce the expression of the pro-apoptotic gene, *grim* (Chen et al., 1996), specifically in the PG in a time controlled manner. We utilized *phantomGAL4* (*phmGAL4*), which exhibits specific expression in the PG within the brain (Supp Fig. 1A). In the whole animal, *phmGAL4* is additionally expressed only in a limited number of carcass cells, as previously described (modENCODE Tissue Expression RNA-seq, Flybase (Roy et al., 2010)) (Supp Fig. 1B). To ensure precise timing of PG apoptosis induction, we incorporated a

temperature-sensitive GAL80 (*phmGAL4tubGAL80^{ts} x UAS-Grim*). Under normal rearing conditions at 18 °C, animals develop without disruption. However, upon shifting the temperature to 29 °C, GAL80's inhibitory function is lost due to its inability to bind GAL4, allowing GAL4 to induce *grim* expression. Consequently, *grim* promotes the apoptosis of the PG (named PGX), preventing further production of ecd (Fig. 1A). This leads to the arrest of developmental progression at the corresponding stage (see Fig. 1A' for timing correspondences with wild-type development). As a control, we employed the induction of a nuclear green fluorescent protein gene, stinger-GFP, in the PG instead of *grim* (*phmGAL4tubGAL80^{ts} x UAS-sti GFP*). With this approach we were able to induce *GAL4>UAS* expression as soon as 4 h after the temperature shift, confirmed by the observation of positive GFP expression in PGs of control animals (Supp Fig. 1C). 4h after temperature shift PGX animals already have several PG cells expressing Death caspase-1 (Dcp-1), a marker of apoptosis (Supp Figs. 1C–D). Consistently, quantification of the maximum intensity of Dcp-1 signal in whole PGs, revealed a significant increase in Dcp-1 staining in PGX when compared to control PGs (Supp Fig. 1E). The increase in Dcp-1 expression is accompanied, as expected, by a decrease in the total number of cells in the PG (Supp Fig. 1F). To further confirm that PG ablation using this method effectively reduces ecd signaling systemically, we quantified the expression of early ecdysone induced genes, Eigs, (Eig71Eb and Eig71Ef as examples) in animals 4h after induction of PG ablation (Supp Fig. 1G). We observed that, at this timepoint, there is a significant decrease in the expression of these genes in PGX animals (*UAS-Grim*). 24h after ablation, the PG is no longer visible (Supp Fig. 1H).

As expected, impeding ecd signaling before CW, blocked developmental progression and these animals continued as growing larvae for up to 12 days (Fig. 1B). A closer analysis of the brain 48 h after PG ablation, a timepoint correspondent to wandering behaviour (48 h Al3e, Fig. 1A'), revealed that the number and size of NBs in PG ablated brains (PGX or *UAS-Grim*) is similar to the brains of control animals (*UAS-sti GFP*) (Fig. 1C–D, J, K). As in controls, NBs in PGX brains are positive for phosphorylated histone 3 (PH3), a marker of proliferative cells (Fig. 1C and D arrows). These results confirm that NBs and their proliferative ability are preserved even in the absence of ecd production.

Interestingly, the analysis of brains at later time points, such as at 72 h AL3e (a timepoint equivalent to 24 h APF) and 7 days AL3e (a time point equivalent to 1 day old adult), revealed that PGX brains have higher number of NBs than controls of the equivalent age (Fig. 1E–H). Consistent with a normal function, the NBs present in these long-lived larvae continue dividing, evidenced by the presence of some NBs in metaphase (Figs. 1I–10 days AL3e, equivalent to a 3 day old adult). Wild-type NBs in pupal stages have been described to progressively reduce their sizes prior to decommissioning (Homem et al., 2014), in contrast, NBs from PGX brains maintain a constant diameter from late L3 (48 h AL3e) until 7 days AL3e (~0 day adult) (Fig. 1C–H, K). This constancy in NB size demonstrates that these NBs are not entering the "shrinkage" program that normally occurs prior to their disappearance in pupal stages (Ito and Hotta, 1992; Truman and Bate, 1988). These results indicate that in the absence of systemic ecd signaling NBs keep dividing for a longer period of time than wild type NBs. Furthermore, it demonstrates that NBs cannot regulate their proliferative window solely in a cell-autonomous manner.

3.2. NB unlimited proliferation capacity is independent of animal nutrition

PGX larvae are arrested as L3 and thus have a prolonged feeding period when compared to wild type animals, that stop eating when they enter the wandering stage and leave the food. The wandering L3 stage thus marks the end of the feeding period of development and the start of metamorphosis, as pupae are nonfeeding and immobile. PGX larvae, however, fail to start wandering behaviour and never form a pupa, which means they have access to food for a longer period of time to promote tissue growth and proliferation. This prompted us to hypothesize that the longer feeding period experienced by PGX animals could be the reason why, in the central brain, NBs continue to proliferate.

To test whether the long NB proliferation time observed in brains of PGX animals (*UAS-grim*) is a consequence of a prolonged feeding period, we subjected these animals to a nutrient starvation regime starting at 48 h AL3e. This timepoint was chosen to mimic the starvation that naturally occurs when wandering behavior starts. The animals were kept in a 5% agar medium for a period of 5 days. The reduction of total body mass after 5 days of nutrient restriction (Fig. 2A) is indicative that the starvation regime was effective. We also observed that 48 h AL3e PGX animals have a higher body mass than control animals of the same age. This is consistent with previous studies that showed that lack of ecd leads to acceleration of larval growth culminating in heavier larvae at the end of L3 development (Colombani et al., 2005).

After 5 days under starvation (7 days AL3e, equivalent to 0 day adult), we observed that brains of PGX animals still have NBs in the central brain, similar to what happens in a fed condition (Fig. 2B and C). The presence of PH3-positive NBs indicates that NBs are mitotically active in brains of both fed and starved animals (Fig. 2B and C). NB number and diameter are also similar in both fed and starved conditions (Fig. 2D and E). These results led us to conclude that the longer NB proliferation observed in brains of animals depleted of ecd is not a consequence of the prolonged feeding period experienced by these animals.

3.3. Ecd depletion during early L3 leads to a reduction of NB division rate

In previous sections we established that the brains of animals with ablated PGs retain mitotically active NBs for as long as 10 days AL3e (Fig. 1I). To investigate whether these long-lived NBs have a similar proliferation profile as control NBs, we next analyzed their mitotic rate by quantifying the percentage of PH3-positive NBs per brain lobe. This analysis revealed that PGX brains have a lower percentage of actively dividing NBs. In wandering, stage, at 48h AL3e, only approximately 10% of NBs are PH3 positive, compared to ~16% in control brains (Fig. 3A). At later timepoints the division rate of NBs in PGX animals remains low, with rates of 8.4% at 72h AL3e, 7.8% at 7 days AL3e, and 8.8% at 10 days AL3e (Fig. 3A).

As PH3 labels cells in mitosis, to further confirm that these NBs are actively cycling and are not stuck in mitosis, we did an additional analysis with 5-Ethynyl-2′-deoxyuridine (EdU), which is incorporated in DNA during replication, S-Phase ("click it" reaction (Salic and Mitchison, 2008);). The successful incorporation of EdU confirms that these cells are indeed cycling (Fig. 3B–G). Consistent with the findings from the PH3 staining analysis, the EdU assay further confirmed that PGX brains generally have a lower number of NBs in S phase across most of the timepoints (Fig. 3B–G). Combined, these results demonstrate that lack of ecd from the beginning of L3 development does not prevent NB division although it leads to a significant reduction in their division rate.

As ablation of the PG prevents ecd synthesis and thus ecd signaling in the entire animal, we next asked if ecd acts directly in NBs to regulate their division rate or if it acts through a non-autonomous mechanism. To answer this question, we specifically disrupted ecd signaling in NBs by either overexpressing a dominant negative form of the ecd receptor (EcR-DN) exclusively in Type I NBs (using AseGAL4; UAS-CD8-GFP) or by knocking down EcR by RNAi in all NBs (using insc-GAL4 UASCD8GFP) since embryonic development. Subsequently, we quantified the mitotic rate of NBs at 48hAL3e (Supp Fig. 2A-D, E, G). These findings show that disrupting the expression of EcR in NBs is sufficient to reduce their mitotic rate thus confirming that reducing ecd signaling directly in NBs is sufficient to reduce NB mitotic rate. In line with the decreased NB proliferation rate, these brains also exhibit a significantly lower number of neurons (Supp Figs. 2F and H). To further confirm the influence of ecd's CW peak on NB proliferation rate, we established primary cell cultures of brain NBs from animals dissected at 0h AL3e

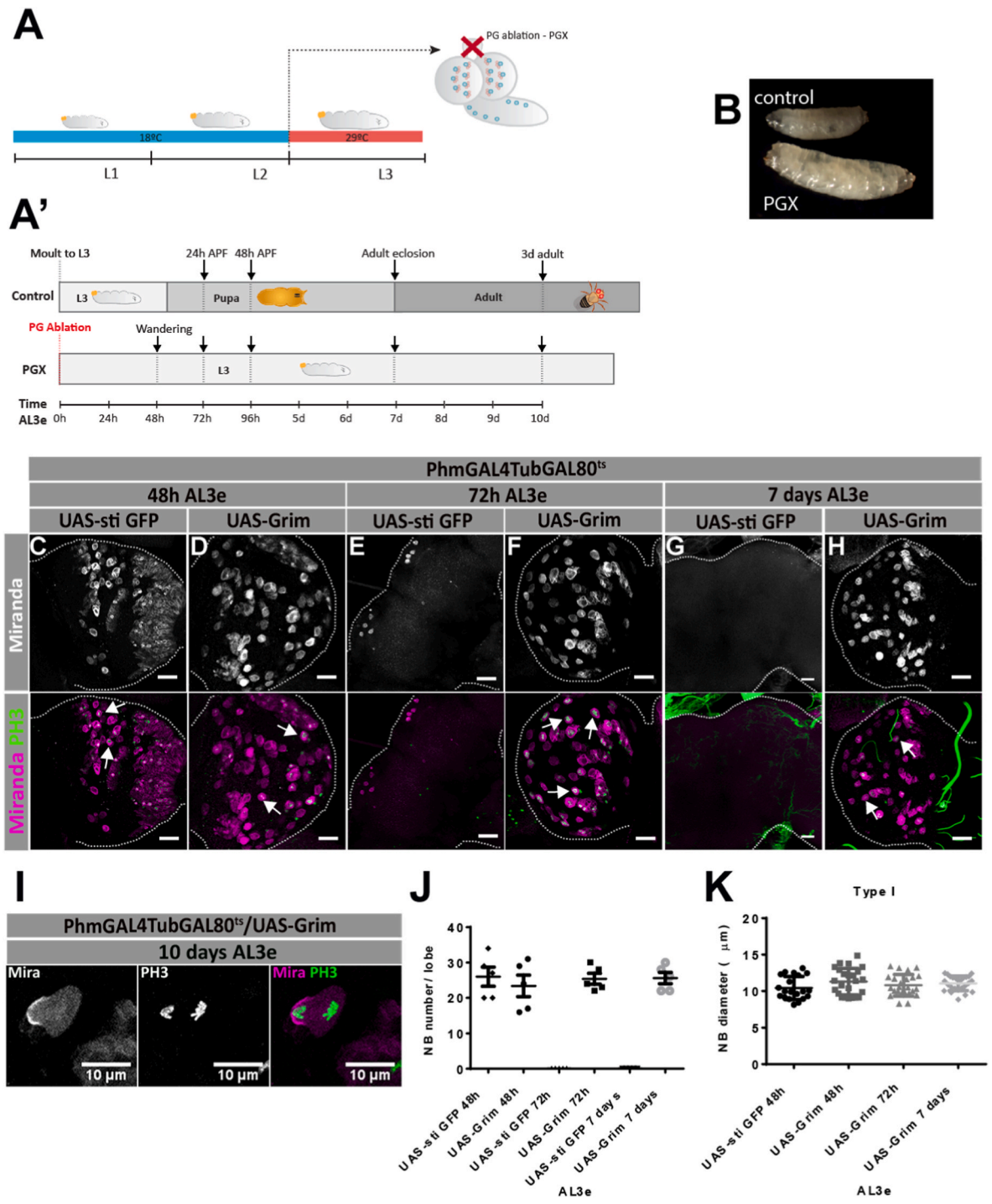

Fig. 1. Ablation of ecdysone production at early L3 stage leads to NBs that do not cease to proliferate

(A) Protocol used for the ablation of the prothoracic gland (PG). Animals developed normally at 18 °C until the moult to L3, when they were shifted to 29 °C to induce apoptosis of the PG (PGX). (A′) Diagram showing equivalent timepoints of control animals and animals with the PG ablated (PGX) at 0 h AL3e. After PG ablation development is arrested. Timepoints analyzed are indicated by the arrows.

(B) Picture of control larva (*PhmGAL4TubGAL80^{ts} x UAS-sti GFP)* at 48hAL3e (top) compared to a *PhmGAL4TubGAL80^{ts} x UAS-Grim* (PGX) larva 12 days AL3e (bottom).

(C–H) Immunofluorescent images of fixed brains lobes of the indicated genotypes at the indicated timepoints. Control brains (*UAS-sti GFP*) compared with brains with PG ablated (*UAS-Grim*) since 0h AL3e. Outlines indicate the edges of the brain lobes. NBs are stained with Miranda (white in the upper panel, and magenta in the lower panel) and phosphorylated histone H3 (PH3 - green, white arrows).

(I) Immunofluorescent image of a dividing NB in a fixed 10-day old PG ablated brain (*UAS-Grim*). NB stained with Miranda (white and magenta) and PH3 (green). Scale bar represents 10 µm.

(J) Quantification of Type I NB number in control (*UAS-sti GFP*) and PG ablated animals (*UAS-Grim*) at the indicated timepoints. n=5 brains for all timepoints.

(K) Quantification of Type I NB diameter throughout time. N= 5 brains for all timepoints.

hAL3e stands for hours after L3 ecdysis, d stands for days, APF stands for after puparium formation. Error bars represent ±SEM. no significance in all conditions, One-Way Anova.

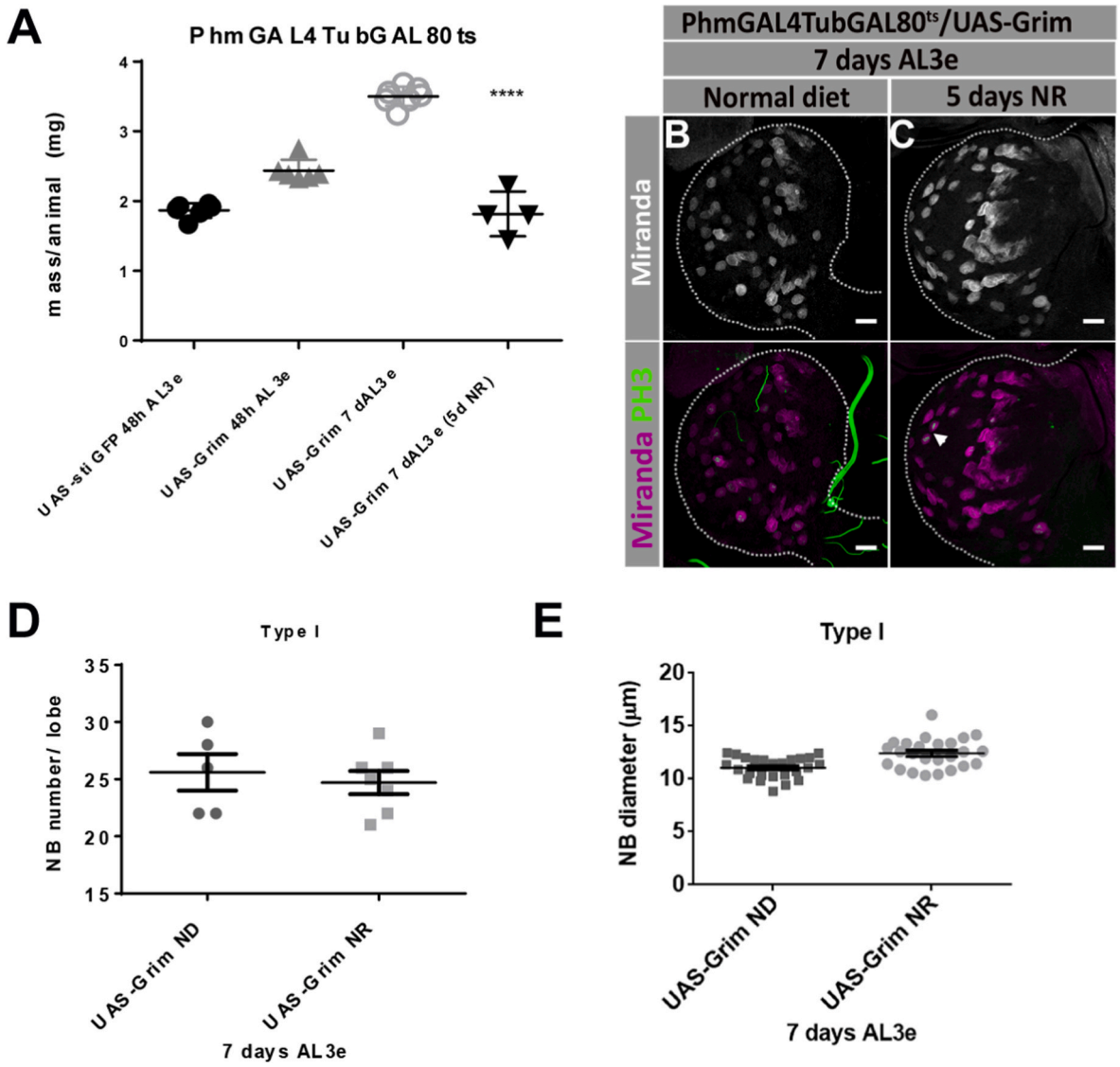

Fig. 2. Animal nutrient restriction does not affect NBs proliferative capacity in ecdysone depleted animals

(A) Quantification of body weight of larvae *PhmGAL4TubGAL80^{ts}* crossed to *UAS-sti GFP* (control) or *UAS-Grim* (PG ablated at 0h AL3e, PGX) at indicated stages in normal diet or nutrient restricted (NR) diet. 5d NR = 5 days in NR diet. Number of animals analyzed: *UAS-sti GFP* 48hAL3e n=6, *UAS-Grim* n=6, *UAS-Grim* 7d AL3 n=6, *UAS-Grim* 7dAL3e NR n=4. One-Way Anova.

(B–C) Immunofluorescent images of fixed brains lobes of the indicated genotype (*UAS-Grim* induced at 0h AL3e) at 7d AL3e under normal diet or under nutrient restriction (NR) for 5 days. NBs are marked with Miranda (white in top panel, magenta in bottom panel) and phosphorylated histone H3 (PH3- green, white arrowhead). Outlines indicate the edges of the brain lobes.

(D) Quantification of central brain type I NB number in brains of animals with PG ablated (*UAS-Grim* at 0h AL3e) nutrient restricted (NR) or fed normal diet (ND). ND n=5 brains, NR n=7 brains. No significance, *t*-test.

(E) Quantification of central brain type I NB diameter in brains of animals with PG ablated (*UAS-Grim* at 0h AL3e) nutrient restricted (NR) or in animals fed under normal diet (ND), ND n=5 brains, NR n=7 brains. No significance, *t*-test.

hAL3e stands for hours after L3 ecdysis, d stands for days. Scale bars represent 20 µm. Error bars represent ±SEM. **** represents P value < 0.0001.

(before the occurrence of the CW peak). We compared the division rate of these NBs when cultured with or without 20-Hydroxyecdysone (20-HE). Consistently, this analysis revealed a significantly lower division rate for NBs cultured without 20-HE compared to those cultured with 20-HE (Fig. 3H and I).

In the previous experiments the PG gland was ablated at the beginning of L3 (Fig. 3J; top scheme, PG ablation at 0h AL3e – end of ecd signaling represented by the end of solid green line), precluding the formation of the CW peak and all ecd peaks after that. Because the different peaks of ecd are able to induce different gene cascades in the same tissue (Guo et al., 2016; Stoiber et al., 2016), we next asked whether ecd regulation of NB mitotic rate occurs in response to a specific ecd peak. To answer this question, we started by testing if it is the 1st L3 peak, the CW peak, that is necessary and sufficient for the regulation of NB proliferation rate. Thus, we let the CW peak occur and ablated the PG right after, preventing the formation of all subsequent peaks of ecd (Fig. 3J; lower scheme, PG ablation at 12h AL3e; Ecd signaling, green line, now occurs until CW is complete). These animals are exposed to the CW peak of ecd, but not any subsequent peaks (Hansson and Lambertsson, 1989). As a result, they do not pupariate and exhibit longer lived, proliferative NBs (Fig. 3K-R). However, NBs from these animals, which have been exposed to the CW peak, divide at a similar rate to control NBs at 48h AL3e and at 72h AL3e (Figs. 3K–48h AL3e (wandering), 72h AL3e (equivalent to 24h APF)). Interestingly, at 7 days

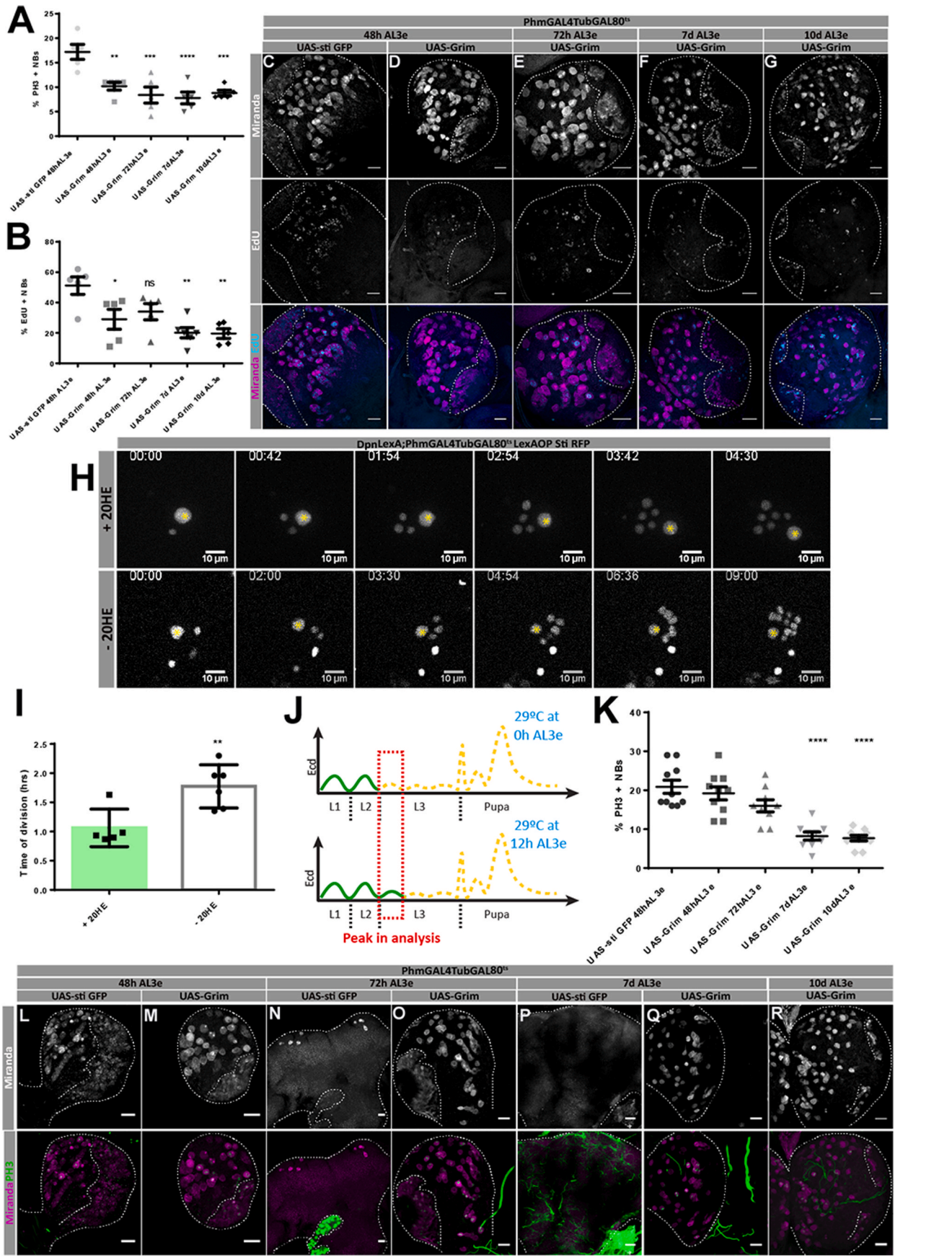

(caption on next page)

Fig. 3. The Critical Weight peak of ecdysone regulates NB mitotic rate.
(A–G) Ablation of the PG was done at 0h hAL3e, before critical weight (CW) peak.
(A) Percentage of phosphorylated histone H3 positive (PH3+) NBs per brain lobe at the indicated developmental times. (*UAS-sti GFP* = *PhmGAL4TubGAL80^{ts} x UAS-sti GFP*, *UAS-Grim* = *PhmGAL4TubGAL80^{ts} x UAS-Grim*) n=5 brains for all timepoints. One-Way Anova.
(B) Percentage of EdU positive NBs per brain lobe at the indicated developmental times. n=5 brains for all timepoints except *UAS-Grim* 7dAL3e for which n=6. One-Way Anova.
(C–G) Immunofluorescent images of fixed brains lobes of the indicated genotypes at the indicated timepoints. Control brains (*UAS-sti GFP*) compared with brains with PG ablated (*UAS-Grim*). NBs are stained with Miranda and EdU. Scale bars represent 20 μm. Outlines indicate the edges of the brain lobes and edges of the optic lobe.
(H) Single frames of time lapse movies of NBs from control animals with the indicated genotype. Brains were dissected and dissociated at 0h hAL3e. Dissociated NBs were cultured with or without 20-hydroxyecdysone (20HE). Yellow asterisk marks the NB. Scale bars represent 10 μm. Time is indicated as hours:minutes.
(I) Quantification of cell cycle times of NBs from control brains with genotype as described in (H), dissected at 0h AL3e and cultured with or without the addition of 20HE. Hrs stands for hours. *t*-test
(J) Scheme of the ablation of the PG before (top scheme, PGX at 0h AL3e) and after the CW peak of ecd (bottom scheme, at 12h AL3e). To analyze the function of the CW peak, ablation of the PG was done at 12h hAL3e, after the occurrence of the CW peak and before the start of the second L3 peak. This way the only additional peak that occurs in this experimental setup is the CW peak, allowing the analysis of its specific effect in NBs. Green line represents the peaks of ecd that occur normally, when the PG is ablated at the indicated timepoint. Dashed yellow line represents the peaks of ecdysone that no longer occur when the PG is ablated at the indicated timepoint. Dashed red square highlights the peak in analysis.
(K–R) Ablation of the PG was done at 12h hAL3e, after the CW peak.
(K) Percentage of PH3+ cells per brain lobe in control brains (*UAS-Sti GFP*) compared with brains with PG ablated since 12h AL3e (*UAS-Grim*) at the indicated developmental times. n= 10 brains for *UAS-sti GFP* and *UAS-Grim* 48hAL3e, n=9 for *UAS-Grim* 72hAL3e and 7dAL3, n=8 for *UAS-Grim* 10dAL3e. One-Way Anova.
(L–R) Immunofluorescent images of fixed brains lobes of the indicated genotypes at the indicated timepoints. Control brains (*UAS-sti GFP*) compared with PG ablated brains (*UAS-Grim*) since 12h AL3e. In panel N the control PG is visible (expressing sti GFP, outlined) Outlines indicate the edges of the brain lobes and the edges of the optic lobes. NBs are stained with Miranda (white in the upper panel, and magenta in the lower panel) and PH3 (green). Scale bars represent 20 μm.
hAL3e stands for hours after L3 ecdysis, d stands for days. Error bars represent ±SEM. * represents P value < 0.05, *** represents P value < 0.001 **** represents P value < 0.0001.

AL3e (equivalent to adult eclosion) NB's mitotic rate decreases to approximately 8%. This suggests the existence of a mechanism that limits NB division if animals continue to fail in completing metamorphosis and adult formation.

These results indicate that the CW peak of ecd is necessary for regulating the proliferation rate of larval NBs. In the absence of this stage specific ecd signal, NBs have a slower rate of proliferation. The CW peak informs the animal that it has reached the minimum viable weight necessary to proceed with metamorphosis. Remarkably, these results indicate that the CW peak also plays a role in organs which do not undergo metamorphosis, such as the brain, where it acts by regulating the division rate of NSCs.

3.4. The ecdysone peak at the transition from larva to pupa, the puparation peak, is responsible for triggering NB shrinkage and neurogenesis termination

Our previous results show that although the CW peak regulates NB mitotic rate, it is not sufficient to trigger the shrinkage and timely decommissioning of NBs, evidenced by the prolonged period of proliferation of these cells (Fig. 3K-R). This suggests that the regulation of NB mitotic rate and overall proliferative window are independent events and thus might be regulated by different ecd peaks. So next we asked whether any of the remaining peaks of ecd is sufficient to trigger NB shrinkage and decommission.

To test whether the ecd peak required for NB decommissioning is any of the remainder peaks that occur during L3 development, we ablated the PG at 32h AL3e, after all of the three small L3 ecd peaks but before the start of the puparation peak (Berreur and Porcheron, 1984; Parvy et al., 2005) (Fig. 4A). We observed that when the PG is ablated at this time point, NBs maintain a constant size and continue dividing until 7d AL3e (Fig. 4B–G). This is similar to the results obtained when the PG was ablated at the start of L3 development or after the CW peak (Figs. 1 and 3). We thus conclude that neither of the three ecd peaks in L3 development are sufficient to inform NBs to start the shrinking process and to terminate proliferating.

Next, we tested the requirement of the puparation peak to trigger NBs decommission. Indeed, the timing of occurrence of this peak coincides with the start of NB size reduction (Homem et al., 2014) suggesting that this might be the peak that triggers the start of this process. We have thus ablated the PG at 0h APF, after the puparation peak occurred (Warren et al., 2006) (the occurrence of the puparation peak was further ensured by the selection of only white prepupae for PG ablation, Fig. 4H). We observed that, at 24h APF, a timepoint when very few NBs are present in the central brain of control animals, PGX brains have a higher number of NBs than control, albeit being as small as control NBs (Fig. 4I, J, M, N). However, shortly after, at 48h APF, NBs are no longer found in the central brain (Fig. 4K, L, M). These results show that NBs that are exposed to the puparation peak start reducing their sizes as normal and are able to exit cell-cycle. Although these NBs exit cell-cycle, this occurs with a delay as they only disappear at 48h APF, in contrast to wild-type NBs which normally decommission at 24h APF. These observations led us to conclude that ecd signaling, specifically the high concentration ecd peak at the transition from L3 to pupal stages, described to induce puparation, is necessary to promote central brain pupal NB shrinking and decommissioning. It additionally suggests that the peaks occurring after the puparation peak might have some contribution in determining the exact timing of NB decommissioning.

3.5. Ecdysone depleted brains have fewer differentiated cells

NBs generate invariable neuronal lineages, so, it is very interesting to explore whether these extended-lifespan NBs produce additional neurons. The majority of central brain NB divisions result in the formation of one ganglion mother cell (GMC) that in turn divides to originate two specialized cells, namely neurons or glia. The total number of differentiated progeny generated depends on the total number of NB divisions, which is influenced by the rate of NB division and the duration of the proliferative period. When ecd signaling is prevented from the start of L3 stage and pre-CW peak, the division rate of NBs decreases, while their proliferative period is significantly prolonged (up to an additional 7 days). So, we next asked how ecd depletion pre-CW ultimately affects the number of differentiated progeny formed.

Using the known neuronal marker embryonic lethal abnormal vision (Elav) (Koushika et al., 1996), we quantified the number of neurons present in brains where the PG was ablated at 0h AL3e, prior to CW peak (Fig. 5A–G). At 48h AL3e (wandering stage), PGX brains have fewer Elav positive cells than control animals, 1608 *vs.* 1940 neurons respectively, although this difference is not significant (Fig. 5N). At 72h AL3e (~24h APF, the timepoint when normally neurogenesis terminates) the number of neurons in PGX brains does not significantly increase when compared to 48h AL3e PGX brains and is much lower than what is observed in

control brains at 72h AL3e (24h APF; 1879 *vs.* 4491 respectively) (Fig. 5N). At 10 days AL3e (~3 day adult) the number of neurons present in PGX brains is 2473, still much lower than the number of neurons in control adult brains (0 day adult, 7d AL3e). These results show that the longer proliferative period observed in NBs in animals with PG ablated pre-CW does not result in the production of an excess number of neurons.

So, could the reduced division rate observed when the PG is ablated pre-CW justify this reduction in the number of neurons? To address this question, we calculated the theoretical ratio of differentiated cells formed by control and PGX NBs, based on experimentally observed division rates at each timepoint (Supp Fig. 3A). Interestingly, PGX NBs are predicted to produce fewer differentiated cells at 48h and 72h AL3e compared to control NBs (Supp Fig. 3A). However, by 7 days AL3e the number of differentiated cells predicted to be generated by PGX NBs should surpass the total number generated by control NBs. However, even after 7 additional days of divisions (10 days AL3e), the number of neurons observed in PGX brains remains significantly lower than in control brains (Fig. 5N). These calculations indicate that the slower division rate observed in PGX NBs is not sufficient to explain the reduced

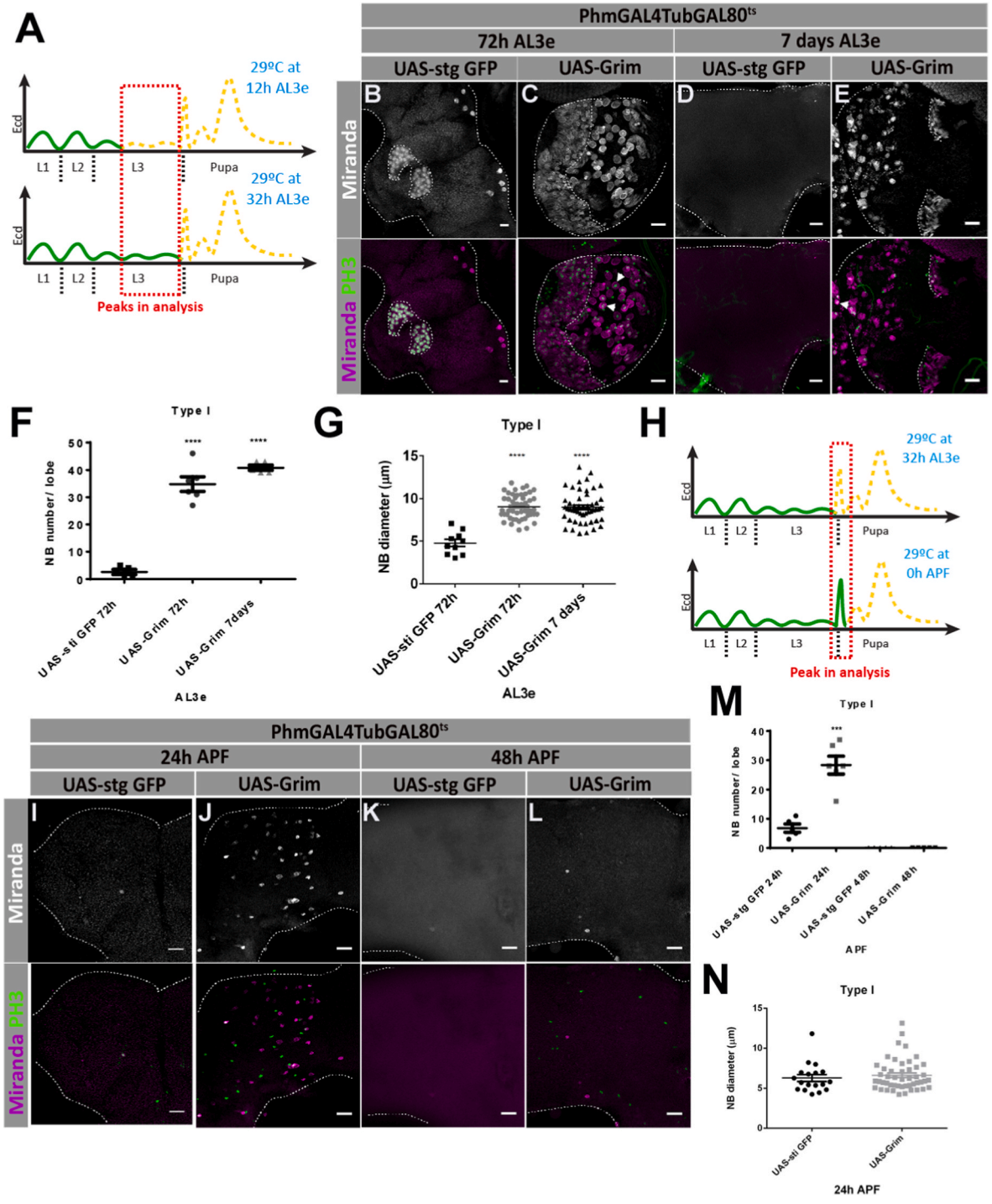

(caption on next page)

Fig. 4. The ecdysone peak at the transition from larva to pupa is responsible for triggering NB shrinkage and decommissioning
(A-G) Ablation of the PG was done at 32h hAL3e, after all L3 peaks of ecd.
(A) Scheme of the ablation of the PG right after CW (top scheme, PGX at 12h AL3e) and after all the three L3 peaks of ecd (bottom scheme, 32h AL3e). To analyze the function of the remaining two L3 peaks of ecd, ablation of the PG was done at 32h hAL3e. This strategy allowed for the 2nd and 3rd L3 peaks to occur, allowing the analysis of their specific effects in NBs. Green line represents the peaks of ecd that occur normally, when the PG is ablated at the indicated timepoint. Dashed yellow line represents the peaks of ecdysone that no longer occur when the PG is ablated at the indicated timepoint. Dashed red square highlights the peak in analysis.
(B–E) Immunofluorescent images of fixed brains lobes of the indicated genotypes at the indicated developmental times. Control brains (*UAS-sti GFP* = *PhmGAL4-TubGAL80^{ts} x UAS-sti GFP*) compared with brains PG ablated at 32h AL3e (*UAS-Grim* = *PhmGAL4TubGAL80^{ts}* x *UAS-Grim*). In panel B the control PG is visible (expressing Sti GFP, outlined). Outlines indicate the edges of the brain lobes and edges of optic lobes. NBs are stained with Miranda (white in the upper panel, and magenta in the lower panel) and phosphorylated histone H3 (PH3 - green).
(F) Quantification of Type I NB number in control (*UAS-sti GFP*) and PG ablated brains (*UAS-Grim*) at the indicated timepoints. n=5 brains for all timepoints. One-Way Anova.
(G) Quantification of Type I NB diameter in control (*UAS-sti GFP*) and PG ablated brains (*UAS-Grim*) at the indicated timepoints. n=5 brains for all timepoints. One-Way Anova.
(H–N) Ablation of the PG was done at 0h APF.
(H) Scheme of the ablation of the PG after the pupariation peak of ecd. To analyze the function of the pupariation peak, ablation of the prothoracic gland was done at 0h APF, after the occurrence of this peak. This strategy allowed for the pupariation peak to occur, allowing the analysis of its specific effects in NBs. Green line represents the peaks of ecd that occur normally, when the PG is ablated at the indicated timepoint. Dashed yellow line represents the peaks of ecdysone that no longer occur when the PG is ablated at the indicated timepoint. Dashed red square highlights the peak in analysis.
(I–L) Immunofluorescent images of fixed brains lobes of the indicated genotypes at the indicated developmental times. Control brains (*UAS-sti GFP*) compared with brains with PG ablated at 0h APF (*UAS-Grim*) at the indicated timepoints. Outlines indicate the edges of the brain lobes. NBs are stained with Miranda (white in the upper panel, and magenta in the lower panel) and PH3 (green).
(M) Quantification of number of Type I NBs in control (*UAS-sti* GFP) and PG ablated brains (*UAS-Grim*), genotypes as in (I–L) at 24h APF and 48h APF (n=5 brains for all timepoints). N=5 all timepoint except *UAS-Grim* 24hAPF for which n=6 brains. One-Way Anova.
(N) Quantification of Type I NB diameter of control (*UAS-sti* GFP) and PG ablated brains (*UAS-Grim*), genotypes as in (I–L) at 24h APF (n=5 brains for all timepoints). No significance, *t*-test.
hAL3e stands for hours after L3 ecdysis, d stands for days. h APF stands for hours after puparium formation. Scale bars represent 20 μm. Error bars represent ±SEM. **** represents P value < 0.0001.

number of differentiate cells in these brains.

To further validate whether the reduced mitotic rate of NBs by itself can account for the decreased number of neurons, we analyzed brains in which the PG was ablated at 12h AL3e, allowing the CW peak to occur normally. Ablation at this stage does not affect NB mitotic rate (Fig. 3). The analysis of these brains revealed that the number of neurons formed is also reduced when compared to control brains (Supp Fig. 3B). This finding confirms that the reduced number of neurons observed is not solely due to lower mitotic rates. It suggests that, the lack of ecd somehow affects the formation and/or maintenance of neurons.

Since NBs also generate glial cells, we investigated if glial cell number is affected when the PG is ablated at 0h AL3e (pre-CW). Using an antibody against reversed polarity (Repo), a common glial marker (Halter et al., 1995), we found that, similarly to neurons, there are fewer glial cells in PGX brains when compared to control brains (Fig. 5H-M, O). This suggests that gliogenesis may also be affected by reduced ecd signaling. However, as glial cells divide multiple times during development (Hartenstein, 2011), we cannot exclude the possibility that glia proliferation is also affected by the lack of ecd signaling.

In conclusion, our findings demonstrate that while the absence of the CW peak of ecd significantly extends the proliferative period of NBs, these brains exhibit a considerable decrease in differentiated cells. Moreover, we conclude that the reduced mitotic rate of these NBs alone cannot account for the observed reduction in the number of differentiated neurons and glia.

3.6. Ecdysone depleted brains have normal levels of apoptosis

A possible explanation for the reduced number of neurons in brains with PGs ablated from pre-CW or from 12h AL3e is that NBs are able to generate intermediate progenitors, but these progenitors fail to divide and generate neurons and glia. Such differentiation defects are known to result in the accumulation of these intermediate cell states within lineages (Eroglu et al., 2014). To test this hypothesis, we quantified the number of intermediate progenitors per NB lineage but found no differences between control and PGX (Supp Fig. 4). This indicates that longer-lived NB lineages exhibit the expected number of intermediate progenitors, thereby ruling out defects in lineage differentiation as an explanation for the diminished number of neurons and glia observed in brains depleted of ecd.

Another possible explanation is that the neurons formed in PGX brains are being eliminated. To test this hypothesis, we quantified the number of apoptotic cells in PGX pre-CW and control brains using an antibody against Dcp-1. As shown in Fig. 6, we found no significant difference in the number of Dcp-1 positive cells at any of the timepoints analyzed (Fig. 6 B). This indicates that the differentiated cells formed by longer-lived NBs are not undergoing excessive apoptosis. In conclusion, our findings demonstrate that ecd signaling during L3 stages plays a crucial role in regulating the development of neurons and glia, influencing the final count of these differentiated cells. However, the decreased number of neurons and glia observed in brains lacking the CW peak of ecdysone cannot be attributed to a blockage in NB lineage differentiation or elevated apoptosis levels.

4. Discussion

The regulation of growth during development is a complex process that involves multiple factors, from cell autonomous to extrinsic factors like environmental conditions to systemic signals such as hormones. In *Drosophila* and in other insects the steroid hormone ecdysone is the major coordinator of developmental transitions, regulating both growth and the cessation of growth at the systemic level. Timed increases in the concentration of ecd, known as ecd pulses, trigger each of the larval molts, and metamorphosis, by triggering the puparium an pupal formations (Andres and Thummel, 1992). Together with other hormones like Insulin, ecd regulates growth to ensure the proportional size of the body and its various organs are reached. In *Drosophila,* the commitment to transition from the growth period to metamorphosis occurs through the attainment of a critical weight in the 3rd larval instar (L3). After this timepoint the body prepares for metamorphosis and, roughly two days later, growth ceases and the animal pupariates, a transition again induced by a pulse of ecd (Berreur et al., 1979). Reaching critical weight changes the way the animals respond to starvation, which no longer results in the delay of metamorphosis. Reaching this milestone is signaled by the release of a small concentration of ecd from the PG, the CW peak. The CW-peak is also known as the commitment-peak since this

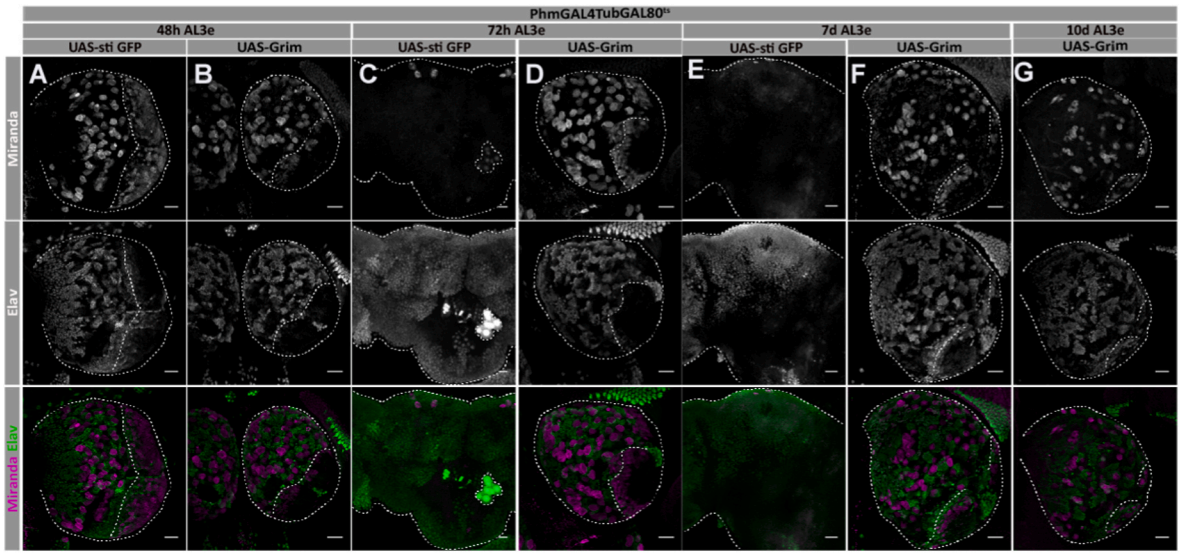

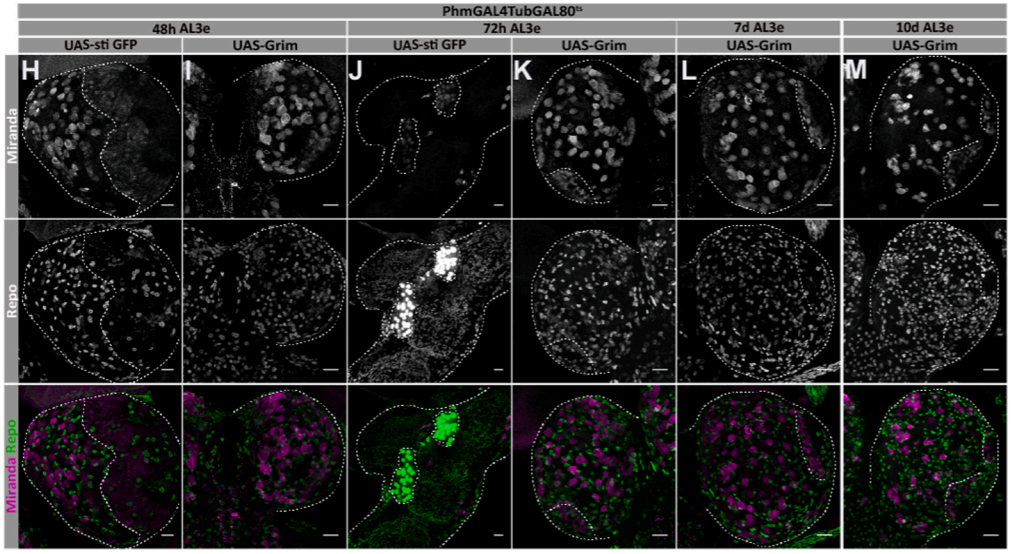

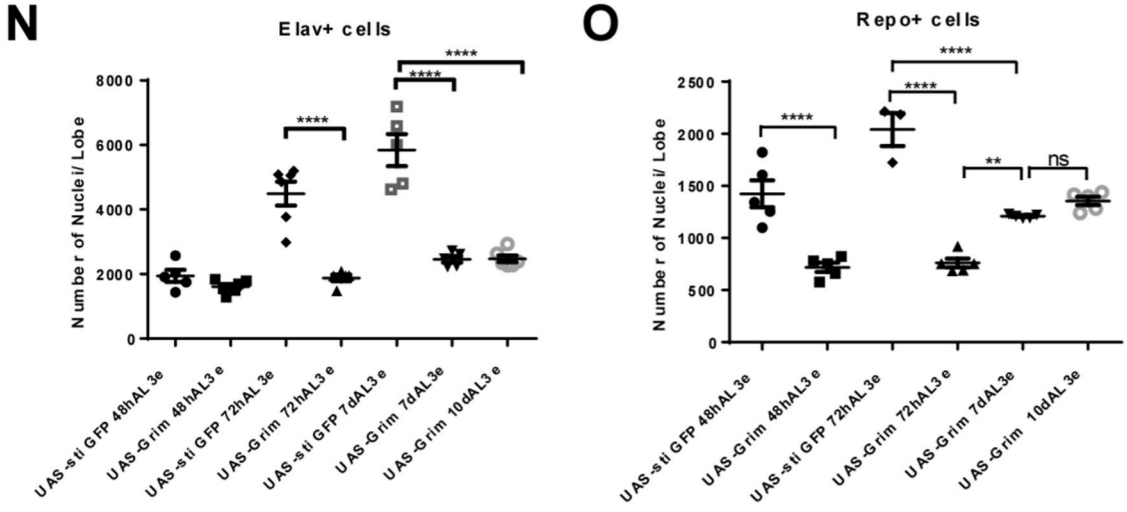

(caption on next page)

Fig. 5. Ecdysone depleted brains have a lower number of differentiated cells
(A-P) Ablation of the PG was done at 0h hAL3e, before CW peak.
(A–G) Immunofluorescent images of fixed brains lobes of the indicated genotypes at the indicated timepoints. Control brains (*UAS-sti GFP* = *PhmGAL4TubGAL80^{ts}* x *UAS-sti GFP*) compared with brains depleted of ecdysone (*UAS-Grim* = *PhmGAL4TubGAL80^{ts}* x *UAS-Grim*). NBs are stained with Miranda (white in the upper panel, and magenta in the lower panel), neurons labelled by embryonic lethal abnormal visual system (Elav - white in the upper panel, green lower panel). On panel C the control PG is visible (expressing Sti GFP, outlined).
(H–M) Immunofluorescent images of fixed brains lobes of the indicated genotypes at the indicated timepoints. Control brains (*UAS-sti GFP*) compared with brains with PG ablated (*UAS-Grim*). NBs are stained with Miranda (white in the upper panel, and magenta in the lower panel) and glia is labelled with reversed polarity (Repo - white in the upper panel, green lower panel). On panel J the control PG is visible (expressing sti GFP, outlined).
(N) Quantification of Elav positive cells per brain lobe at the indicated timepoints, genotypes as indicated in H-M (n=5 brains for *UAS-sti GFP* 48hAL3e, *UAS-sti GFP* 72hAL3e, 7d AL3e and *UAS-Grim* 7d AL3e, n=6 brains for *UAS-Grim* 48hAL3e, 72h AL3 and 10dAL3e).
(O) Quantification of Repo positive cells per brain lobe at the indicated timepoints, genotypes as indicated in H-M (n=5 brains for all genotypes except *UAS-sti GFP* 72hAL3e for which n=3).
hAL3e stands for hours after L3 ecdysis, d stands for days. Error bars represent ±SEM. Scale bars represent 20 μm. Ns=non significance, ** represents P value < 0.01, **** represents P value < 0.0001, One-Way Anova.

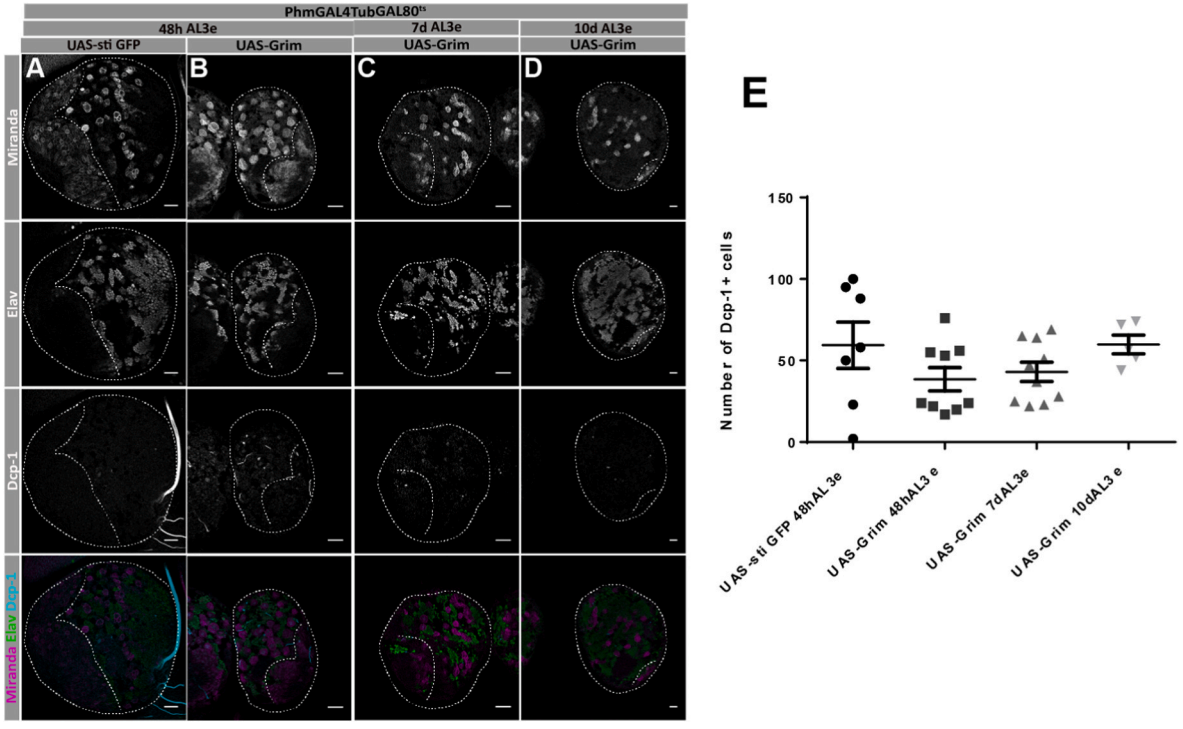

Fig. 6. Ecdysone depleted brains have normal levels of apoptosis
(A-E) Ablation of the PG was done at 0h hAL3e, before the CW peak.
(A–D) Immunofluorescent images of fixed brains lobes of the indicated genotypes at the indicated timepoints. Control brains (*UAS-sti GFP* = *PhmGAL4TubGAL80^{ts} x UAS-sti GFP*) compared with PG ablated brains (*UAS-Grim* = *PhmGAL4TubGAL80^{ts} x UAS-Grim*). NBs are stained with Miranda (white in the upper panel, and magenta in the lower panel), neurons labelled by embryonic lethal abnormal visual system (Elav, white in the upper panel, green lower panel) and Death caspase-1 (Dcp-1 - white in the third panel, cyan in the lower panel). Outlines indicate the edges of the brain lobes and the edges of the optic lobes.
(E) Quantification of Dcp-1 positive cells per brain lobe at the indicated timepoints, genotypes as indicated in A-D (n=7 brains for *UAS-sti GFP* 48hAL3e, n= 9 brains for *UAS-Grim* 48hAL3e, n=10 brains for *UAS-Grim* 7d AL3e and n=5 for *UAS-Grim* 10d AL3e).
hAL3e stands for hours after L3 ecdysis, d stands for days. Scale bars represent 20 μm. Error bars represent ±SEM. No significance, One-Way Anova.

signal will commit larvae to metamorphose without delay (De Moed et al., 1999).

Ecd also regulates the growth of tissues and organs throughout the L3 stage. In late L3, ecd promotes cell cycle progression in the wing disc (Mitchell et al., 2008) where it is also required to determine its growth and final size (Alves et al., 2022; Herboso et al., 2015; Strassburger et al., 2021). In contrast, ecd induces programmed cell death in other larval tissues such as the larval midgut or the larval salivary glands (Hara et al., 2013), while it is not required for the growth of the larval gut (Herboso et al., 2015). At the end of larval development, ecd promotes the histolysis of most of the larval tissues and induces growth arrest of imaginal discs that will undergo metamorphosis during pupal stages (Guo et al., 2016). Thus, the role of ecd is both stage and tissue specific.

The different organs that grow during the L3 stage, differ in their sensitivity to nutrition at different stages of development. For instance, starving early L3 larvae significantly compromises wing disc growth (Mirth and Shingleton, 2012; Shingleton et al., 2007), while starving them later in L3 development has a milder effect. (Shingleton et al., 2008). In the brain, during L1 and early L2 stages, nutrition is essential to induce NB exit from quiescence and to ensure the beginning of larval/secondary neurogenesis. During L3, NB proliferation is maintained, independently of animal nutrition, by a constitutively active Alk, a tyrosine kinase that can activate downstream targets of the insulin pathway in the absence of insulin like peptides (Cheng et al., 2011). Thus, during late larval development, starvation does not lead to a large reduction in brain growth as it does in other organs (Brogiolo et al., 2001; Hietakangas and Cohen, 2009; Lanet et al., 2013; Puig et al., 2003). This is called the brain-sparing phenomenon and ensures that, at

the end of development, a functional brain with a minimal number and variety of neurons is formed (Cheng et al., 2011; Lanet et al., 2013). Exactly when or how this Alk-mediated starvation protection starts remains unclear (reviewed in Lanet and Maurange, 2014).

As brain growth mainly depends on NB proliferation, we asked how ecd coordinates body growth with NB proliferation. By doing timed ablations of the PG at different timepoints during the L3 stage, we allowed the formation of only certain pulses of ecd to determine what is their specific function in the regulation of NBs (Fig. 7). We found that the first ecd peak in L3 development, the CW peak, acts as a developmental checkpoint for central brain NBs, regulating their mitotic rate such that, in the absence of this peak, they have longer cell cycle time. As the CW-peak signals the point when the animal reaches the minimum viable weight required to survive metamorphosis, these results for the first time demonstrate that the brain, which does not undergo metamorphosis, is also subject to this developmental checkpoint. This occurs, possibly to ensure that the adult brain is formed at the same pace as the rest of the body, thus protecting the functionality of the adult animal. It is interesting to speculate that the CW-peak could also serve as a checkpoint for the start of brain sparing in starvation conditions. Several links between ecd signaling and cell-cycle have been previously reported in other contexts. For instance, high levels of ecd induces cell cycle arrest in *Drosophila* cell culture lines (Stevens et al., 1980). In the wing disc, ecd's pupariation peak has been shown to induce Broad, which in turn results in repression of String and a temporary G2 cell cycle arrest in the wing (Guo et al., 2016). The role of ecd here observed in pre-CW NBs goes however in a different direction, suggesting that ecd's regulatory role of cell-cycle is likely tissue and stage specific. The exact mechanism by which ecd regulates NB cell cycle remains an interesting open question.

Our PG ablation experiments have also revealed that the high concentration pulse of ecd that triggers pupariation is the peak responsible for neurogenesis termination. Although previous experiments had implicated ecd in the process of decommissioning (Homem et al., 2014), for technical reasons it was then not possible to identify which of the ecd peaks was responsible for the for this process. Here we show that the pupariation peak is the one required to induce NB size reduction and decommissioning. Interestingly, despite having the information to terminate neurogenesis, these NBs are delayed in their time of decommission which suggest that they are missing some of the information required to know exactly when to exit cell cycle. This additional signal might come from the small peak of ecd that occur right after the pupariation peak (D'Avino and Thummel, 1998). This peak occurs around 12h APF and is responsible for the induction of pupation, limb extension and head eversion. It would not be farfetched to speculate that this peak also acts in NBs to coordinate cell cycle exit with this developmental milestone. Nonetheless, these results interestingly show that termination of neurogenesis is nicely coordinated with pupariation of the animal and the end of the growth period. Our results show that,

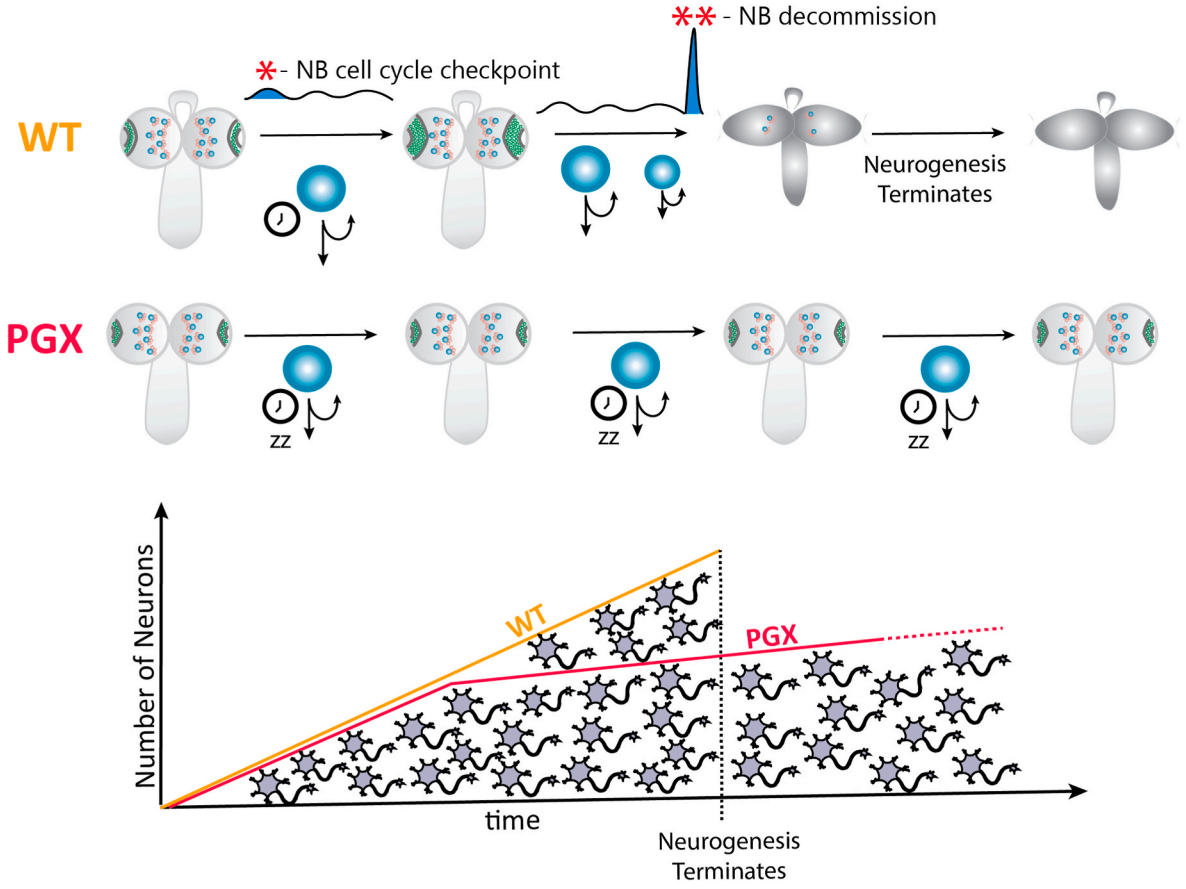

Fig. 7. Model

In wild type animals (WT), larval central brain NBs proliferate at a certain pace, regrowing to their original size after each division. The critical weight peak (CW) of ecd, at the start of L3 development (*) is necessary to determine the pace at which larval NBs divide. Later, at the transition from larval to pupal development, ecdysone is again required, through the high concentration peak that induces pupariation (**), to signal NBs to start the progressive size reduction that culminates cell cycle exit and termination of neurogenesis. We propose ecdysone has thus two opposite roles in the regulation of brain development: First by promoting NB division in early L3, when CW is attained and later on, at the start of metamorphosis, to trigger the process that leads to NB proliferation exit.

In ecdysone depleted animals pre-CW (PGX) NBs proliferate at slower rate but for an indefinite time. Although these NBs divide for a much longer period, these brains have less differentiated neurons, revealing an important role for ecdysone signaling in neuron maintenance. The reduction in neuron number is not due to increased levels of apoptosis nor lineage differentiation defects.

when ecd is absent throughout L3 development, central brain NBs continue to proliferate for up to 7 days longer (168 h) then their wild-type counterparts. This increase in NB lifespan is enormous, representing more than double of their normal lifespan (from L1 to pupa, wild-type larval NBs can divide a maximum of 120 h). Normally NBs form invariable lineages with the same number and fate of neural progeny. These results show however, that NBs have the intrinsic capacity to proliferate indefinitely. These data place ecd hormonal signaling hierarchically upstream of cell-autonomous NB fate regulation mechanisms such as the temporal transcription factor series (Brody and Odenwald, 2000; Isshiki et al., 2001), as in the absence of ecd, the cell-autonomous transcriptional network is not sufficient for the regulation of the proliferative window of NBs.

One of the most unexpected results is that in the absence of ecd signaling, despite NBs having a longer proliferative period, brains have a significantly lower number of neurons and glia. This shows that ecd signaling during L3 is required for the correct maintenance or generation of neurons. The reduction in neuron number in PG ablated brains cannot be however solely explained by slower cell cycle pace of NBs, as animals where the PG gland was ablated post-CW peak, in which case NBs have a normal cell cycle pace, still have a lower number of neurons. As we found no obvious defects in central brain NB lineage differentiation, this phenotype does not seem to be caused by a defect in neuron generation either. We quantified apoptosis levels in these brains to test for the hypothesis that the neurons being generated were eliminated by apoptosis but found no differences. It has been recently described that disrupting ecd pathway in the optic lobe leads to defects in dendritic, axonal processes and synaptic connectivity (Jain et al., 2022). Could ecd be necessary upon neuron generation to activate signals that promote neuron activity and thus their maintenance? Or could the fate of these newly formed neurons be "wrong" making them unable to form the right connections which could lead to their elimination in an apoptosis-independent mechanism? The precise molecular mechanism that acts downstream of ecd to maintain neurons remains an open question.

In summary, here we report that ecd regulates brain development at two different stages by differentially regulating the proliferation properties of NBs. We show that the CW-peak, at the start of L3 stage, regulates larval NB cell cycle pace. We also demonstrate that the pupariation peak of ecd is responsible for terminating the NB proliferative period and neurogenesis. Our results additionally show that, at the cellular level, *Drosophila* neural stem cells have an intrinsic capacity to proliferate indefinitely, placing ecd hormonal signaling hierarchically upstream of the cell-autonomous NB temporal fate regulation. We also show that ecd is required to ensure the brain has the correct number of neurons and glial cells. Ultimately, our study reveals new insights on how the coordination of brain growth with whole body development requires the regulation of stem cell proliferation by developmental cues.

Author contributions

AO designed and performed experiments, data analysis, design of data analysis, figure assembly and wrote the manuscript. CH did conceptual design of the study, designed experiments, assisted figure assembly and wrote the manuscript. All authors contributed to the article and approved the submitted version.

Funding

This project has received funding from the European Research Council (ERC) under the European Union's Horizon 2020 research and innovation programme (H2020-ERC-2017-STG-GA 759853-StemCell-Habitat); by Wellcome Trust and Howard Hughes Medical Institute (HHMI-208581/Z/17/Z-Metabolic Reg SC fate); EMBO Installation grant (H2020-EMBO-3311/2017/G2017); by Fundação para a Ciência e Tecnologia (PTDC/BIA-BID/0681/2021 IF/01265/2014/CP1252/CT0004 and PD/BD/136895/2018 to AO). Nova Medical School was funded by iNOVA4Health—UIDB/04462/2020 and UIDP/04462/2020, and by the Associated Laboratory LS4FUTURE (LA/P/0087/2020), two programs financially supported by Fundação para a Ciência e Tecnologia/Ministério da Ciência, Tecnologia e Ensino Superior. The Fly facility was funded by CONGENTO LISBOA-01-0145-FEDER- 022170.

Declaration of competing interest

The authors declare that the research was conducted in the absence of any commercial or financial relationships that could be construed as a potential conflict of interest.

Data availability

Data will be made available on request.

Acknowledgements

We thank Christen Mirth, Takashi Koyama and César Mendes for fly stocks and Jürgen Knoblich for the Miranda antibody. We also thank Nova Medical School's Microscopy and Fly facilities for technical support.

Stocks obtained from the Bloomington *Drosophila* Stock Center (NIH P40OD018537) were used in this study. The monoclonal antibodies were obtained from the Developmental Studies Hybridoma Bank, created by the NICHD of the NIH and maintained at The University of Iowa, Department of Biology, Iowa City, IA 52242.

Appendix A. Supplementary data

Supplementary data to this article can be found online at https://doi.org/10.1016/j.ydbio.2023.08.001.

References

Alves, A.N., Oliveira, M.M., Koyama, T., Shingleton, A., Mirth, C.K., 2022. Ecdysone coordinates plastic growth with robust pattern in the developing wing. Elife 11, 1–24. https://doi.org/10.7554/eLife.72666.

Andres, A.J., Thummel, C.S., 1992. Hormones, puffs and flies: the molecular control of metamorphosis by ecdysone. Trends Genet. 8, 132–138. https://doi.org/10.1016/0168-9525(92)90371-A.

Bello, B.C., Izergina, N., Caussinus, E., Reichert, H., 2008. Amplification of neural stem cell proliferation by intermediate progenitor cells in Drosophila brain development. Neural Dev. 3, 5. https://doi.org/10.1186/1749-8104-3-5.

Berreur, P., Porcheron, P., 1984. Ecdysteroids during the third larval lnstar in/(3) ecd-lfs , a mutant of Drosophila melanogaster. Gen. Comp. Endocrinol. 84, 76–84.

Berreur, P., Porcheron, P., Berreur-Bonnenfant, J., Simpson, P., 1979. Ecdysteroid levels and pupariation in drosophila melanogaster. J. Exp. Zool. 210, 347–352. https://doi.org/10.1002/jez.1402100218.

Boulan, L., Andersen, D., Colombani, J., Boone, E., Léopold, P., 2019. Inter-organ growth coordination is mediated by the Xrp1-dilp8 Axis in Drosophila. Dev. Cell 49, 811–818.e4. https://doi.org/10.1016/j.devcel.2019.03.016.

Brody, T., Odenwald, W.F., 2000. Programmed transformations in neuroblast gene expression during Drosophila CNS lineage development. Dev. Biol. 226, 34–44. https://doi.org/10.1006/dbio.2000.9829.

Brogiolo, W., Stocker, H., Ikeya, T., Rintelen, F., Fernandez, R., Hafen, E., 2001. An evolutionarily conserved function of the Drosophila insulin receptor and insulin-like peptides in growth control. Curr. Biol. 11, 213–221. https://doi.org/10.1016/S0960-9822(01)00068-9.

Chen, P., Nordstrom, W., Gish, B., Abrams, J.M., 1996. grim, a novel cell death gene in Drosophila. Genes Dev. 10, 1773–1782. https://doi.org/10.1101/gad.10.14.1773.

Cheng, L.Y., Bailey, A.P., Leevers, S.J., Ragan, T.J., Driscoll, P.C., Gould, A.P., 2011. Anaplastic lymphoma kinase spares organ growth during nutrient restriction in drosophila. Cell 146, 435–447. https://doi.org/10.1016/j.cell.2011.06.040.

Colombani, J., Andersen, D.S., Léopol, P., 2012. Secreted peptide dilp8 coordinates Drosophila tissue growth with developmental timing. Science 80 (336), 582–585. https://doi.org/10.1126/science.1216689.

Colombani, J., Bianchini, L., Layalle, S., Pondeville, E., Dauphin-Villemant, C., Antoniewski, C., Carré, C., Noselli, S., Léopold, P., 2005. Antagonistic actions of ecdysone and insulins determine final size in Drosophila. Science 84 310, 667–670. https://doi.org/10.1126/science.1119432.

D'Avino, P.P., Thummel, C.S., 1998. Crooked legs encodes a family of zinc finger proteins required for leg morphogenesis and ecdysone-regulated gene expression

during Drosophila metamorphosis. Development 125, 1733–1745. https://doi.org/10.1242/DEV.125.9.1733.
De Moed, G.H., Kruitwagen, C.L.J.J., De Jong, G., Scharloo, W., 1999. Critical weight for the induction of pupariation in Drosophila melanogaster: genetic and environmental variation. J. Evol. Biol. 12, 852–858. https://doi.org/10.1046/j.1420-9101.1999.00103.x.
Droujinine, I.A., Perrimon, N., 2016. Interorgan communication pathways in physiology: focus on Drosophila. Annu. Rev. Genet. 50, 539–570. https://doi.org/10.1146/annurev-genet-121415-122024.
Eroglu, E., Burkard, T.R., Jiang, Y., Saini, N., Homem, C.C.F., Reichert, H., Knoblich, J. A., 2014. SWI/SNF complex prevents lineage reversion and induces temporal patterning in neural stem cells. Cell 156, 1259–1273. https://doi.org/10.1016/J.CELL.2014.01.053.
Garelli, A., Gontijo, A.M., Miguela, V., Caparros, E., Dominguez, M., 2012. Imaginal discs secrete insulin-like peptide 8 to mediate plasticity of growth and maturation. Science 84 336, 579–582. https://doi.org/10.1126/science.1216735.
Guo, Y., Flegel, K., Kumar, J., Mckay, D.J., Buttitta, L.A., 2016. Ecdysone signaling induces two phases of cell cycle exit in *Drosophila* cells. Biol. Open 5, 1648–1661. https://doi.org/10.1242/bio.017525.
Halter, D.A., Urban, J., Rickert, C., Ner, S.S., Ito, K., Travers, A.A., Technau, G.M., 1995. The homeobox gene repo is required for the differentiation and maintenance of glia function in the embryonic nervous system of Drosophila melanogaster. Development 121, 317–332. https://doi.org/10.1242/DEV.121.2.317.
Hansson, L., Lambertsson, A., 1989. Steroid regulation of glue protein genes in Drosophila melanogaster. Hereditas 110, 61–67. https://doi.org/10.1111/j.1601-5223.1989.tb00418.x.
Hara, Y., Hirai, K., Togane, Y., Akagawa, H., Iwabuchi, K., Tsujimura, H., 2013. Ecdysone-dependent and ecdysone-independent programmed cell death in the developing optic lobe of Drosophila. Dev. Biol. 374, 127–141. https://doi.org/10.1016/j.ydbio.2012.11.002.
Hartenstein, V., 2011. Morphological diversity and development of glia in Drosophila. Glia 59, 1237–1252. https://doi.org/10.1002/glia.21162.
Herboso, L., Oliveira, M.M., Talamillo, A., Pérez, C., González, M., Martín, D., Sutherland, J.D., Shingleton, A.W., Mirth, C.K., Barrio, R., 2015. Ecdysone promotes growth of imaginal discs through the regulation of Thor in *D. melanogaster*. Sci. Rep. 5, 12383 https://doi.org/10.1038/srep12383.
Hietakangas, V., Cohen, S.M., 2009. Regulation of tissue growth through nutrient sensing. Annu. Rev. Genet. 43, 389–410. https://doi.org/10.1146/annurev-genet-102108-134815.
Homem, C.C.F., Reichardt, I., Berger, C., Lendl, T., Knoblich, J.A., 2013. Long-term live cell imaging and automated 4D analysis of Drosophila neuroblast lineages. PLoS One 8. https://doi.org/10.1371/journal.pone.0079588.
Homem, C.C.F., Steinmann, V., Burkard, T.R., Jais, A., Esterbauer, H., Knoblich, J.A., 2014. Ecdysone and mediator change energy metabolism to terminate proliferation in drosophila neural stem cells. Cell 158, 874–888. https://doi.org/10.1016/j.cell.2014.06.024.
Isshiki, T., Pearson, B., Holbrook, S., Doe, C.Q., 2001. Drosophila neuroblasts sequentially express transcription factors which specify the temporal identity of their neuronal progeny. Cell 106, 511–521. https://doi.org/10.1016/S0092-8674(01)00465-2.
Ito, K., Hotta, Y., 1992. Proliferation pattern of postembryonic neuroblasts in the brain of Drosophila melanogaster. Dev. Biol. 149, 134–148. https://doi.org/10.1016/0012-1606(92)90270-Q.
Jain, S., Lin, Y., Kurmangaliyev, Y.Z., Valdes-Aleman, J., Locascio, S.A., Mirshahidi, P., Parrington, B., Zipursky, & S.L., 2022. A global timing mechanism regulates cell-type-specific wiring programmes. Naturen 603. https://doi.org/10.1038/s41586-022-04418-5.
King, R.C., Aggarwal, S.K., Bodenstein, D., 1966. The comparative submicroscopic morphology of the ring gland of Drosophila melanogaster during the second and third larval instars. Z. für Zellforsch. Mikrosk. Anat. 73, 272–285. https://doi.org/10.1007/BF00334868.
Koushika, S.P., Lisbin, M.J., White, K., 1996. ELAV, a Drosophila neuron-specific protein, mediates the generation of an alternatively spliced neural protein isoform. Curr. Biol. 6, 1634–1641. https://doi.org/10.1016/S0960-9822(02)70787-2.
Koyama, T., Rodrigues, M.A., Athanasiadis, A., Shingleton, A.W., Mirth, C.K., 2014. Nutritional control of body size through FoxO-Ultraspiracle mediated ecdysone biosynthesis. Elife 3, 1–20. https://doi.org/10.7554/eLife.03091.
Lanet, E., Gould, A.P., Maurange, C., 2013. Protection of neuronal diversity at the expense of neuronal numbers during nutrient restriction in the Drosophila visual system. Cell Rep. 3, 587–594. https://doi.org/10.1016/j.celrep.2013.02.006.
Lanet, E., Maurange, C., 2014. Building a brain under nutritional restriction: insights on sparing and plasticity from Drosophila studies. Front. Physiol. https://doi.org/10.3389/fphys.2014.00117.
Livak, K.J., Schmittgen, T.D., 2001. Analysis of relative gene expression data using real-time quantitative PCR and the 2-ΔΔCT method. Methods 25, 402–408. https://doi.org/10.1006/meth.2001.1262.
Maurange, C., Cheng, L., Gould, A.P., 2008. Temporal transcription factors and their targets schedule the end of neural proliferation in Drosophila. Cell 133, 891–902. https://doi.org/10.1016/j.cell.2008.03.034.
Mirth, C.K., Shingleton, A.W., 2012. Integrating body and organ size in Drosophila: recent advances and outstanding problems. Front. Endocrinol. 3, 1–13. https://doi.org/10.3389/fendo.2012.00049.
Mitchell, N., Cranna, N., Richardson, H., Quinn, L., 2008. The Ecdysone-inducible zinc-finger transcription factor Crol regulates Wg transcription and cell cycle progression in Drosophila. Development 135, 2707–2716. https://doi.org/10.1242/DEV.021766.
Neufeld, T.P., De La Cruz, A.F.A., Johnston, L.A., Edgar, B.A., 1998. Coordination of growth and cell division in the Drosophila wing. Cell 93, 1183–1193. https://doi.org/10.1016/S0092-8674(00)81462-2.
Nijhout, H.F., Riddiford, L.M., Mirth, C., Shingleton, A.W., Suzuki, Y., Callier, V., 2014. The developmental control of size in insects. Wiley Interdiscip. Rev. Dev. Biol. https://doi.org/10.1002/wdev.124.
Oldroyd, H., 1951. Biology of Drosophila. Nature. https://doi.org/10.1038/168803a0.
Parvy, J.P., Blais, C., Bernard, F., Warren, J.T., Petryk, A., Gilbert, L.I., O'Connor, M.B., Dauphin-Villemant, C., 2005. A role for βFTZ-F1 in regulating ecdysteroid titers during post-embryonic development in Drosophila melanogaster. Dev. Biol. 282, 84–94. https://doi.org/10.1016/j.ydbio.2005.02.028.
Petavy, G., David, J.R., Gibert, P., Moreteau, B., 2001. Viability and rate of development at different temperatures in Drosophila: a comparison of constant and alternating thermal regimes. J. Therm. Biol. 26, 29–39. https://doi.org/10.1016/S0306-4565(00)00022-X.
Puig, O., Marr, M.T., Ruhf, M.L., Tjian, R., 2003. Control of cell number by Drosophila FOXO: downstream and feedback regulation of the insulin receptor pathway. Genes Dev. 17, 2006–2020. https://doi.org/10.1101/GAD.1098703.
Quinn, L., Lin, J., Cranna, N., Lee, J.E.A., Mitchell, N., Hannan, R., 2012. Steroid hormones in Drosophila: how ecdysone coordinates developmental signalling with cell growth and division. Steroid–Basic Sci. 149–168. https://doi.org/10.5772/27927.
Roy, S., Ernst, J., Kharchenko, P.V., Kheradpour, P., Negre, N., Eaton, M.L., Landolin, J. M., Bristow, C.A., Ma, L., Lin, M.F., Washietl, S., Arshinoff, B.I., Ay, F., Meyer, P.E., Robine, N., Washington, N.L., Di Stefano, L., Berezikov, E., Brown, C.D., Candeias, R., Carlson, J.W., Carr, A., Jungreis, I., Marbach, D., Sealfon, R., Tolstorukov, M.Y., Will, S., Alekseyenko, A.A., Artieri, C., Booth, B.W., Brooks, A.N., Dai, Q., Davis, C.A., Duff, M.O., Feng, X., Gorchakov, A.A., Gu, T., Henikoff, J.G., Kapranov, P., Li, R., MacAlpine, H.K., Malone, J., Minoda, A., Nordman, J., Okamura, K., Perry, M., Powell, S.K., Riddle, N.C., Sakai, A., Samsonova, A.A., Sandler, J.E., Schwartz, Y.B., Sher, N., Spokony, R., Sturgill, D., van Baren, M., Wan, K.H., Yang, L., Yu, C., Feingold, E., Good, P., Guyer, M., Lowdon, R., Ahmad, K., Andrews, J., Berger, B., Brenner, S.E., Brent, M.R., Cherbas, L., Elgin, S.C. R., Gingeras, T.R., Grossman, R., Hoskins, R.A., Kaufman, T.C., Kent, W., Kuroda, M. I., Orr-Weaver, T., Perrimon, N., Pirrotta, V., Posakony, J.W., Ren, B., Russell, S., Cherbas, P., Graveley, B.R., Lewis, S., Micklem, G., Oliver, B., Park, P.J., Celniker, S. E., Henikoff, S., Karpen, G.H., Lai, E.C., MacAlpine, D.M., Stein, L.D., White, K.P., Kellis, M., Booth, B., Comstock, C.L.G., Dobin, A., Drenkow, J., Dudoit, S., Dumais, J., Fagegaltier, D., Ghosh, S., Hansen, K.D., Jha, S., Langton, L., Lin, W., Miller, D., Tenney, A.E., Wang, H., Willingham, A.T., Zaleski, C., Zhang, D., Acevedo, D., Bishop, E.P., Gadel, S.E., Jung, Y.L., Kennedy, C.D., Lee, O.K., Linder-Basso, D., Marchetti, S.E., Shanower, G., Nègre, N., Grossman, R.L., Auburn, R., Bellen, H.J., Chen, J., Domanus, M.H., Hanley, D., Heinz, E., Li, Z., Meyer, F., Miller, S.W., Morrison, C.A., Scheftner, D.A., Senderowicz, L., Shah, P.K., Suchy, S., Tian, F., Venken, K.J.T., White, R., Wilkening, J., Zieba, J., Nordman, J.T., Orr-Weaver, T.L., DeNapoli, L.C., Ding, Q., Eng, T., Kashevsky, H., Li, S., Prinz, J.A., Hannon, G.J., Hirst, M., Marra, M., Rooks, M., Zhao, Y., Bryson, T.D., Perry, M.D., Kent, W.J., Lewis, S.E., Barber, G., Chateigner, A., Clawson, H., Contrino, S., Guillier, F., Hinrichs, A.S., Kephart, E.T., Lloyd, P., Lyne, R., McKay, S., Moore, R.A., Mungall, C., Rutherford, K.M., Ruzanov, P., Smith, R., Stinson, E.O., Zha, Z., Artieri, C.G., Malone, J.H., Jiang, L., Mattiuzzo, N., Feingold, E.A., Good, P.J., Guyer, M.S., Lowdon, R.F., 2010. Identification of functional elements and regulatory circuits by Drosophila modENCODE. Science 330, 1787–1797. https://doi.org/10.1126/SCIENCE.1198374.
Salic, A., Mitchison, T.J., 2008. A chemical method for fast and sensitive detection of DNA synthesis in vivo. Chem. CELL Biol. 105, 2415–2420.
Shingleton, A.W., Frankino, W.A., Flatt, T., Nijhout, H.F., Emlen, D.J., 2007. Size and shape: the developmental regulation of static allometry in insects. Bioessays 29, 536–548. https://doi.org/10.1002/BIES.20584.
Shingleton, A.W., Mirth, C.K., Bates, P.W., 2008. Developmental model of static allometry in holometabolous insects. Proc. R. Soc. B Biol. Sci. 275, 1875–1885. https://doi.org/10.1098/rspb.2008.0227.
Stevens, B., Alvarez, C.M., Bohman, R., O'Connor, J.D., 1980. An ecdysteroid-induced alteration in the cell cycle of cultured Drosophila cells. Cell 22, 675–682. https://doi.org/10.1016/0092-8674(80)90543-7.
Stoiber, M., Celniker, S., Cherbas, L., Brown, B., Cherbas, P., 2016. Diverse hormone response networks in 41 independent Drosophila cell lines. genes genomes Genet 6, 683–694.
Strassburger, K., Lutz, M., Müller, S., Teleman, A.A., 2021. Ecdysone regulates Drosophila wing disc size via a TORC1 dependent mechanism. Nat. Commun. 12, 1–12. https://doi.org/10.1038/s41467-021-26780-0.
Thummel, C.S., 1996. Flies on steroids–Drosophila metamorphosis and the mechanisms of steroid hormone action. Trends Genet. 12, 306–310. https://www.cell.com/trends/genetics/fulltext/0168-9525(96)10032-9.
Truman, J.W., Bate, M., 1988. Spatial and temporal patterns of neurogenesis in the central nervous system of Drosophila melanogaster. Dev. Biol. 125, 145–157. https://doi.org/10.1016/0012-1606(88)90067-X.
Warren, J.T., Yerushalmi, Y., Shimell, M.J., O'Connor, M.B., Restifo, L.L., Gilbert, L.I., 2006. Discrete pulses of molting hormone, 20-hydroxyecdysone, during late larval development of Drosophila melanogaster: correlations with changes in gene activity. Dev. Dynam. 235, 315–326. https://doi.org/10.1002/dvdy.20626.
White, K., Kankel, D.R., 1978. Patterns of cell division and cell movement in the formation of the imaginal nervous system in Drosophila melanogaster. Dev. Biol. 65, 296–321. https://doi.org/10.1016/0012-1606(78)90029-5.